



Stockholm
University

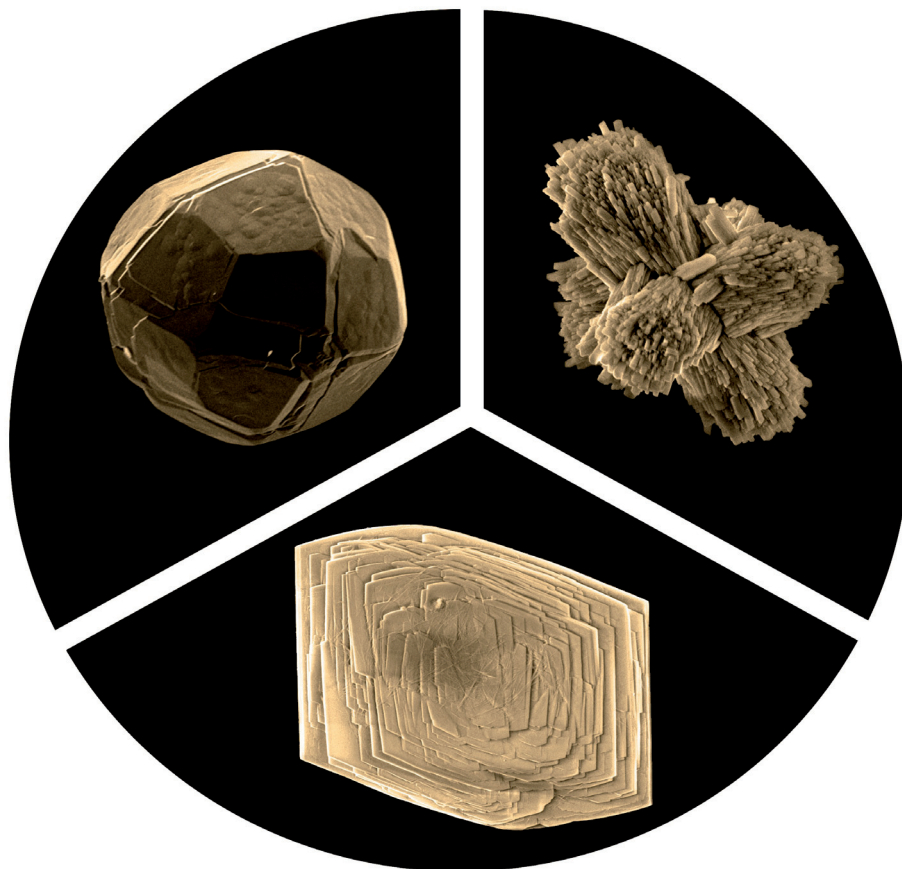
Bachelor Thesis

Degree Project in
Geochemistry 30 hp

Synthesis and characterisation of natural hydrothermal zeolites and their catalysis in N-fixation

An experimental approach

Christoffer Hemmingsson



Stockholm 2013

Department of Geological Sciences
Stockholm University
SE-106 91 Stockholm

Acknowledgements

Thank you to my supervisor Nils Holm for giving me the opportunity to be part of this project. Many thanks to the introduction of instruments & analyses and help during this project to my second supervisor Enrique Iñigues. Also regards to the help using ESEM: Marianne Ahlbom, PXRD & FTIR: Henrik Skogby at NRM, BET: Zoltan Bacsik at material chemistry. The aid in ammonia analysis: Jörgen Ek at ITM. Also thank you to the staff and master students at IGV for general aid and encouragement.

Abstract	4
Sammanfattning	4
Introduction	5
<i>The Hadean</i>	5
<i>Role of zeolites</i>	6
<i>Aims</i>	6
Materials and methods	8
<i>Zeolite characterisation</i>	8
<i>Optical microscopy</i>	8
<i>Environmental Scanning Electron Microscopy (ESEM)</i>	8
<i>Post synthesis Fe-incorporation</i>	9
<i>PXRD</i>	9
<i>Fourier Transform Infrared spectroscopy (FTIR)</i>	9
<i>Specific area BET</i>	10
<i>Catalytic reaction conditions</i>	10
<i>Ammonia analysis</i>	12
<i>C-compounds</i>	12
<i>Statistics</i>	13
Results	14
<i>ESEM</i>	14
<i>PXRD</i>	17
<i>FT-IR</i>	19
<i>BET</i>	20
<i>Catalysis</i>	21
<i>N-analysis</i>	21
<i>C-Analysis</i>	22

Discussion	22
References	25
Appendix	28
1.1 - <i>Dunnett T3, zeolite & iron in situ synthesis</i>	28
1.2 - <i>Dunnett T3, Phillipsite treatments</i>	31
1.3 - <i>Dunnett T3, Analcime treatments</i>	32
1.4 - <i>Dunnett T3, Sanidine treatments</i>	34
2.1 - <i>PXRD, Phillipsite & iron in situ</i>	35
2.2 - <i>PXRD, crystallographic information, phillipsite</i>	36
2.3 - <i>PXRD, Analcime & iron in situ</i>	37
2.4 - <i>PXRD, crystallographic information, analcime</i>	38
2.5 - <i>PXRD, Sanidine & iron in situ</i>	39
2.6 - <i>PXRD, crystallographic information, sanidine</i>	40
3.1.1 - <i>FTIR: Phillipsite & iron in situ</i>	41
3.1.2 - <i>FTIR: Phillipsite & iron in situ - pyridine</i>	41
3.1.3 - <i>FTIR: Phillipsite post synthesis treated - pyridine</i>	42
3.2.1 - <i>FTIR: Analcime & iron in situ - pyridine</i>	43
3.2.2 - <i>FTIR: Analcime & iron in situ - pyridine</i>	43
3.2.3 - <i>FTIR: Analcime post synthesis treated - pyridine</i>	44
3.3.1 - <i>FTIR: Sanidine & iron in situ</i>	45
3.3.2 - <i>FTIR: Sanidine & iron in situ - pyridine</i>	45
3.3.3 - <i>FTIR: Sanidine post synthesis treated - pyridine</i>	46
3.4 - <i>Infra red band assignation table.</i>	47
4.1 - <i>BET Pore volume</i>	48
4.2 - <i>BET Pore surface area</i>	48
4.3 - <i>BET Pore diameter</i>	49

Abstract

The abiotic chemistry to form the components necessary for the origin of life are thought to have emerged during the Hadean eon. It is thought to be characterised by a CO₂/N₂ atmosphere, a shallow acidic ocean with alkaline waters in hydrothermal systems, and a basaltic ocean crust. One of the necessary components for life is bioavailable N-sources such as NH₄. In this study the synthesis of three common natural zeolites was attempted. These were characterised using optical microscopy, ESEM, PXRD, FT-IR and BET. The products synthesised were two zeolites, phillipsite and analcime as well as the feldspar sanidine. These were then also synthesised with an *in situ* Fe²⁺ & Fe³⁺ source in alkaline conditions and the products were exposed to a post-synthesis treatment of de-aluminising and were subjected to iron substitution. Incorporating iron into the crystal structure by replacing Al. Characterisation show that analcime, phillipsite, sanidine and merlinoite were produced. All products, including those with post-synthesis treatments show the presence of Brønsted acid sites. The surface area for iron *in situ* synthesised products show a trend of increasing surface area and pore area/volume when iron is incorporated into the crystal structure. Phillipsite and analcime with their iron *in situ* products were then used in catalysis of N-reduction using a continuous flow system and an autoclave system. The catalysis was run at pH 10 & 100°C to imitate mild hydrothermal conditions. It was seen that analcime had the highest production rate of NH₄⁺; nevertheless, both products were able to produce NH₄⁺ from NO₃⁻, as well as N₂. This gives a new insight into Hadean hydrothermal systems and their role in production of bioavailable N-sources for the origin of life.

Sammanfattning

Abiotisk kemi för att producera komponenter nödvändiga för livets ursprung tros ha framkommit under den Hadeiska eonen. Hadeiska eonen tros vara karakteriserad av en CO₂/N₂ atmosfär, ett grunt och surt hav med alkalint vatten utströmmande från hydrotermala system, samt en basaltisk oceanskorpa. En av de nödvändiga ämnena för liv är biologiskt tillgängliga kväve källor såsom NH₄⁺. I denna studie tillämpades syntes av 3 zeoliter vanligt förekommande i hydrotermala system. Dessa var karakteriserade med optisk mikroskopi, ESEM, PXRD, FT-IR samt BET. Produkterna som syntetiserades var två zeoliter, phillipsit och analcim, samt fältspaten sanidin. Syntesmetoden från dessa produkter användes sedan för att syntetisera mineralen med Fe²⁺ & Fe³⁺ *in situ* i alkalina förhållanden. Efter syntesen behandlades produkterna för att avlägsna aluminium samt substituera aluminium med Fe³⁺ joner. Karakterisering av järn *in situ* produkterna visar en produktion av mineralerna phillipsit, analcim, sanidin och merlinoit. Alla produkter, inklusive post-syntes påvisade Brønstedt acid sites. BET analys för järn *in situ* syntetiserade produkter visar en trend av ökad ytarea, porarea/volym när järn är inkluderat i kristallstrukturen. Phillipsit och analcim samt respektive Fe²⁺ & Fe³⁺ *in situ* produkter användes i katalysreaktion av reducering av N₂, genom att använda ett kontinuerligt flödes system, samt ett autoklav system. Katalyserna skedde vid pH 10 & 100°C för att imitera milda hydrotermala förhållanden. Det visades att analcim hade den största produktionen av NH₄⁺, dock har både phillipsit och analcim möjligheten att katalysera produktionen av NH₄⁺ från både NO₃⁻ samt N₂. Detta ger en ny insikt i hadeiska hydrotermala system och deras roll i produktionen av biotillgängliga kväveresurser för livets ursprung.

Introduction

The Hadean

The Hadean eon (> ~3.8 Ga), was characterised of the formation of the core, and the chemical separation of the lower and upper mantle, occurring in the first 30 Ma together with the formation of the solar system (Trail *et al.* 2013). The hadean atmosphere has been postulated to not be a reducing one, causing an issue as the formation of reduced nitrogen with a CO₂/N₂ atmosphere would be rather difficult. One source of ammonia, starts with the formation of NO from N₂ by shock heating. The NO reacts with HCO (produced photochemically) to HNO that is deposited into oceans via precipitation and forming nitrites and then further reduced by ferrous iron. The ammonia can then turn into ammonium under acidic conditions or even exposed to photochemical destruction in the atmosphere (Summers 1999).

The hadean ocean may have been a carbonic acidic ocean pH ~5, where hydrothermal vents could act as shelters against as alkaline waters pours out through them around pH ~11. These hydrothermal mounds with precipitates of clays, amorphous silica, carbonates, iron sulphides and hydroxides would provide shelter between the two water masses promoting a proton exchange gradient. In a relatively stable environment as such, the potential for chemosynthesis in combination with low temperatures at 100-120°C could promote the formation of life (Nitschke & Russell 2009, Martin *et al.* 2008). In the case not all necessary compounds are available in a single hydrothermal mound, one needs to consider the importance of ocean transport. Though the transport may be slow, this could still supply the boost needed for the synthesis (Stüeken *et al.* 2013). It is indicated that the water on earth comes from three major resources: hydrogen trapped in earth's mantle, II: Water rich bodies from carbonaceous meteorites and comets (Javoy 2005). Supporting the idea there was a water source present in the hadean.

The Hadean crust has been suggested to be more basaltic rather than komatiitic as the presence of zircons found indicate a more silica rich environment, favouring felsic derivatives from basalt over Mg-rich komatiite (Taylor and McLennan 2009). With the development of new micro-analytical abilities, a new study of Titanium on such zircons support the suggestion of a more basaltic hadean earth, as the study suggests earth may have contained either a stable hydrosphere, near/water-saturated granitic magmas or volcanic emissions with volatiles such as CO₂, H₂O and SO₂. Indicating that earth may have had the ability of supporting life ~200 Myr after it's formation (Trail *et al.* 2013).

The bioavailability of nitrogen sources would be important on the early earth as the fixation of N₂ into ammonia would be a key step to be able to form molecules such as amino acids, required for the formation of DNA / RNA, and proteins. To this, it has been hypothesised that the levels of ferrous iron (Fe²⁺), SO₄²⁻ and NO₂⁺ / NO₃⁺ were all important in prebiotic chemistry (Singireddy *et al.* 2012). Processes known today capable of N-reduction in mild conditions are that of bacteria and some legumes able to produce ammonia from air and water.

Ammonia and ammonium (NH₃ and NH₄⁺) are precursors for reactions requiring N-sources in prebiotic synthesis where the efficiency in organic synthesis is more efficient in both aqueous and gaseous environments with NH₃/NH₄⁺ than with N₂. The strecker synthesis is one example where nitrogen is needed to form the intermediary step for the synthesis of amino acids (Smirnov *et al.* 2008).

Several possible pathways to abiotic formation of NH₃/NH₄⁺ has been suggested, such as the reduction of NO₂⁻/NO₃⁻ by Fe²⁺/FeS in the ocean (Smirnov *et al.* 2008). Using modelling, Fe-centers are able to hold both N₂ and N₃-ligands at a single binding site, which may be critical to iron catalytic cycles (Hendrich *et al.* 2006). Atmospheric production

from N₂ and HCN, release from rocks and minerals, photo reduction on mineral surfaces (Smirnov *et al.* 2008), and hydrothermal reduction from N₂ in hydrothermal systems at the presence of minerals in lithospheric settings at temperatures and pressures of 300-800°C and 0.1-0.4 GPa (Brandes *et al.* 1998). This study yielded 17 mol% of N₂ reduced to NH₃ at the very most (at 700°C & 0.1 GPa). (Brandes *et al.* 1998). The synthesis of ammonia from aqueous NO₂ and NO₃ using pyrite has also been seen. Where NO₂ was converted into NO and NH₄⁺ at 70°C and 120°C in μmol kg⁻¹, while NO₃ was reduced only at 120°C. (Singireddi *et al.* 2012). The reduction of N-species into ammonium has also been reported in the presence of Fe⁰ and Ni⁰ at 200, 70 and 22°C, reporting values such as 187, 3.6 and 0.7 μmol NH₄⁺ kg⁻¹ Fe⁰ used (Smirnov *et al.* 2008). The study however also point out the conversion of nitrate and nitrite into ammonium is more efficient than the conversion of N₂. This suggested ammonium can be present in submarine hydrothermal systems that are expected to exist in the Hadean. It is also reported that Fe-containing minerals such as pyrite is important in the context of prebiotic chemistry. As pyrite can be used to reduce NO₂ and NO₃ into ammonia at ambient temperatures of 22-120°C and at pH values greater than 7.5 (Singireddy *et al.* 2012).

The common denominator of all these studies are:

- Nitrates and nitrites are converted into ammonium, particularly at high temperatures. The reduction of these are possible in the presence of pyrite
- Reduction of N₂ in presence of iron is possible, in particularly at high temperatures (Smirnov *et al.* 2008).
- A production of ammonia from N₂ at ambient temperatures and low pressure is still to be reported with confidence.

Role of zeolites

Zeolites are crystalline hydrated aluminosilicates commonly containing group IA and IIA elements in the periodic table (e.g. Na & K, and Mg & Ca respectively), as well as the occasional ferric iron. The variety of zeolites are caused by different ways that silica-tetrahedra link together and which additional elements occupying the spaces between these tetrahedra. When these zeolites are dehydrated, channels in the crystal structure become more accessible, enabling the adsorption of molecules small enough to access the pore spaces (Kesraoui-Ouki *et al.* 1994). The importance of these channels is the distinctive property of being organophilic and hydrophobic (Schoonen *et al.* 2004). Some properties of interest in zeolites are: 1) the ability to exchange cations, 2) the ability to have strong acid sites, 3) The presence of pores in different sizes (Csicsery 1984). Thus being able to act as a source of sink for precursors in chemical reactions and may potentially have played an important role in prebiotic systems (Schoonen *et al.* 2004). On early earth, zeolites should have been present at the ocean floor and hydrothermal systems, through the alteration of ocean crust (Rao *et al.* 1980).

A previous study showed the production of cytosine and adenine (both amino acids needed for the formation of DNA), by reacting CO and NH₃ in the presence of zeolites at 250-325°C (Rao *et al.* 1980). There is however no study showing the production of NH₄ from N₂ using zeolites, to supply this N-source.

Aims

The aims of this project is to synthesise zeolite minerals. These are Analcime, Phillipsite and Clinoptilolite, all three are minerals present in the alteration of seafloor and hydrothermal systems (Schoonen *et al.* 2004). To synthesise products with an *in situ* iron

source as well as modification of the minerals post-synthesis with de-aluminising and the substitution of Al in the zeolite framework with Iron.

The zeolites are then to be characterised with Optical microscopy, ESEM, PXRD, FT-IR, and BET. The presence of Brønsted acid sites in the crystals will be investigated with FT-IR, treating the crystals with pyridine.

The zeolites are then to be used in catalysis reactions at alkaline conditions and ambient temperature of 100°C, to mimic the environment of a mild or shallow hydrothermal system. The experiments are run for 24 h using a flow catalysis set-up and non-site specific catalysis in autoclaves. The presence of NH_4^+ is investigated with ammonium analysis. Samples are also investigated for the presence of organic compounds with GCMS.

Materials and methods

Synthesis of zeolites were guided using references that acquired the desired mineral through synthesis (Table 1). Reaction mixtures were prepared using a Si-solution (Na / K & Silica) heated to $\sim 80^{\circ}\text{C}$, and an Al-solution (Na / K & Aluminium). In the case an iron source was included, solution was stirred with Al and Fe until homogeneous before NaOH & KOH was added) heated to 50°C to ensure both solutions are fully dissolved. The amount of iron added to a solution replaces 5% molar weight of Aluminium, according to a previous successful study (Doula 2007). The Si-solution is then slowly added to the Al-solution during stirring and stirred for 5 min before stopped, upon which the synthesis starts by increasing the temp $10\sim 15^{\circ}\text{C h}^{-1}$ until desired temperature was achieved, using automatic autoclaves at pH 12-13.

Table 1: Gram weight of compound used in pre-reaction mixture. (1: Chen *et al.* 2002, 2: Tatlier *et al.* 2007 , 3: Satokawa & Itabashi 1997)

Synthesis	SiO ₂	Al(OH) ₃	NaOH	KOH	FeCl ₂ • 4H ₂ O	FeCl ₃ • 6H ₂ O	Time, h	Temp, °C
Phillipsite¹								
1	2	0.49	4	5.6	0	0	72	200
2	2	0.33	4	5.6	0.275	0	72	200
3	2	0.33	4	5.6	0	0.32	72	200
Analcime²								
4	2	0.3	4	0	0	0	72	140
5	2	0.19	4	0	0.26	0	72	140
6	2	0.19	4	0	0	0.299	72	140
Clinoptilolite³								
7	2	0.52	0	3.14	0	0	72	195
8	2	0.44	0	3.14	0.29	0	72	195
9	2	0.44	0	3.14	0	0.34	72	195

Zeolite characterisation

Optical microscopy

Each product and modified product was investigated in optical microscope, using plain backlit light at x60 magnification to ensure a generally homogenous sample has been achieved and the crystal form does not change with modification.

Environmental Scanning Electron Microscopy (ESEM)

Scanning electron microscopy (FEI, Quanta FEG 650) was used to further investigate homogeneity and crystal shape of the product. Elemental analysis (EDS / AZtech) was conducted at high vacuum, 20 kV with an Oxford, X-Max detector, at a 10 mm working distance, without X-ray cone. The AZtec mapping function was used with 5 scans for each selected surface, giving average relative elemental composition.

Post synthesis Fe-incorporation

Samples of each non-iron containing product were treated to incorporate iron into the crystal structure, post-synthesis. 0.2 g of Phillipsite, Analcime and Sanidine were exposed to three treatments, to incorporate iron through direct substitution with aluminium, or de-aluminising the crystals before treating with an iron solution. The solutions used were $\sim 8 \times 10^{-3}$ mol/l Fe-solution ($\text{FeCl}_3 \cdot 6\text{H}_2\text{O}$ in MilliQ), 3M HNO_3 , and 5.5×10^{-3} mol/l ammonium bicarbonate (NH_4HCO_3 in MilliQ) solution. The three treatments were:

- I. Substitution: 0.2 g of product were saturated in 3 ml of Fe-solution over night at $\sim 40^\circ\text{C}$.
- II. De-aluminising + incorporation: 0.2 g of product was acid washed with 3 ml of HNO_3 for 5 minutes in ultra sonic bath, two times. The crystals were then extracted and saturated in 3 ml Fe-solution over night $\sim 40^\circ\text{C}$.
- III. De-aluminising + incorporation: 0.2 g of product was saturated in 3 ml of NH_4HCO_3 over night at $\sim 40^\circ\text{C}$. The crystals were then extracted and treated with 3 ml of Fe-solution over night $\sim 40^\circ\text{C}$.

PXRD

Powder X-ray diffraction patterns were obtained using a PANalytical Xpert-Pro diffractometer, at room temperature. The instrument was run at 45 kV and 40 mA at 1.5438 Å wavelength, using Cu-K α radiation and Ni-filter. The samples were then analysed between $5\text{-}40^\circ$ in step sizes of 0.017° in a continuous scan mode with rotation of the sample. The spectra given was then compared to reference spectra to give a percentage match of crystallinity, according to the following equation by Kim & Chung (2003):

$$\text{Crystallinity (\%)} = \frac{\text{peak area of product}}{\text{peak area of reference}} \times 100$$

Fourier Transform Infrared spectroscopy (FTIR)

FTIR is useful in studying structural features of the material due to its sensitivity to the Si/Al-framework (Ming & Boettinger 2001). In particular when iron is present in the structure; however, due to the large amount of atoms in the structure of zeolites, the specific peaks for each can be hard to see (Doula 2007). In this case, the Si/Al-framework is investigated as well as the acidity in the form of Brønstedt acid sites through the bonding of pyridine. As the bonding of pyridine can be seen as a shift in the stretching vibrations of the crystal structure (Dzwigaj *et al.* 2000). Samples are dried at 400°C for 6 h to rid of water in the structure. 0.1 grams of each product is then saturated with $200 \mu\text{l } 10^{-1} \text{ mol l}^{-1}$ pyridine in n-hexane. The samples were left to react with pyridine for 3 days and left to dry in fume hood for 1 day before analysis.

Samples were then ground in an agatha mortar with KBr (99.99%) at an $\sim 10\%$ and 90% ratio, respectively. The material was then pressed into a self supporting pellet placed inside the chamber of a Bruker, Equinox 55 FT-IR, with continuous flushing of dry air. Analysis was conducted at room temperature between $400\text{-}4400 \text{ cm}^{-1}$ wavelengths, resolution 2 cm^{-1} and 20 integrations. The spectra were then compared to reference spectra for Si-Al, Al-O, Si-O, and OH stretching as these can be used to some degree at wavelengths between $400\text{-}4000 \text{ cm}^{-1}$ (Ríos & Williams 2008).

Specific area BET

As zeolites are considered porous materials where the molecular structure / channel network of the zeolite characterises its properties. Gas adsorption is used to characterise these solids, in particular physisorption. That is the physical adsorption of molecules to the surface of the material, creating a thin film due to the physical forces of interaction between gas and material, used to determine the surface area and pore distribution. As for zeolites, a general rule is degassing is required at $\sim 300^{\circ}\text{C}$ (Rouquerol *et al.* 1994). The estimation of surface area is determined by calculations based on the adsorption and desorption of gas, known as BET, that is the Brunauer-Emmett Theory (Brunauer *et al.* 1938). The samples were prepared/analysed using a Micromeritics ASAP2020 volumetric adsorption analyser. Samples were degassed with dynamic vacuum conditions with N_2 at 300°C for 6 h. The recording of adsorption-desorption isotherms occurred submerged in liquid nitrogen, with an internal temperature of $\sim -196^{\circ}\text{C}$. The Specific surface area was then calculated according to the BET method by Brunauer *et al.* (1938), in this case $P/P^0 = 0.05-0.15$ while submerged in liquid nitrogen, recording adsorption-desorption isotherms at -196°C . The Total pore volume was calculated at a relative pressure of P/P_0 0.988 with micro pore volume calculated according to Barret *et al.* (1951) with pore size distribution obtained with a single-point t-plot.

Catalytic reaction conditions

Two catalytic systems are used. The continuous flow system, pushing the reaction through the sample in the furnace, while the remaining system is cold. The second system is autoclaves, this is a rough system with a less controlled environment as the whole solution is heated. This system can be used to say whether ammonia can be produced; however, not pinpoint the production solely on the catalytic properties of the sample.

The continuous flow system (Fig 1) is comprised entirely of stainless steel (316L alloy), except for the boron silica bottle with teflon cap holding the stock solution. The output volume of the LC-pump was maintained at 3 ml min^{-1} , with furnace at 200°C for sample blanks and at 100°C for samples. Stock solution consists of filtered (10 μm glass filter) degassed ultra pure water (MilliQ) while submerged in ultrasonic bath, with KOH to achieve pH 10. As alkaline conditions are more representative for a hydrothermal system (Nitschke & Russell 2009) and KOH may be beneficial in the catalysis of ammonium, as potassium- and ammonium ions have a similar ionic radius and charge, allowing for easier substitution (Schoonen *et al.* 2004) and an iron surface promoted with K^+ is common when it comes to the production of ammonia from N_2 (Rodriguez *et al.* 2011). Stock solution was prepared with combinations of SDT ($\text{Na}_2\text{S}_2\text{O}_4$, sodium dithionite) and KNO_3 at 10^{-2} and 10^{-3} m l^{-1} respectively. The headspace of the stock solution bottle was $\sim 28.25 \text{ cm}^3$.

The reaction conditions of the autoclaves contain the same amounts of solutions and products as those samples in the continuous flow. Rather than stainless steel, the autoclave is lined with a teflon beaker and sealed tight. The head space of both set ups was then flushed by vacuum before filled with N-gas (99.999%), and then vacuumed again and filled with N-gas if needed. An approximate 2 bar N_2 gas was fitted in the headspace.

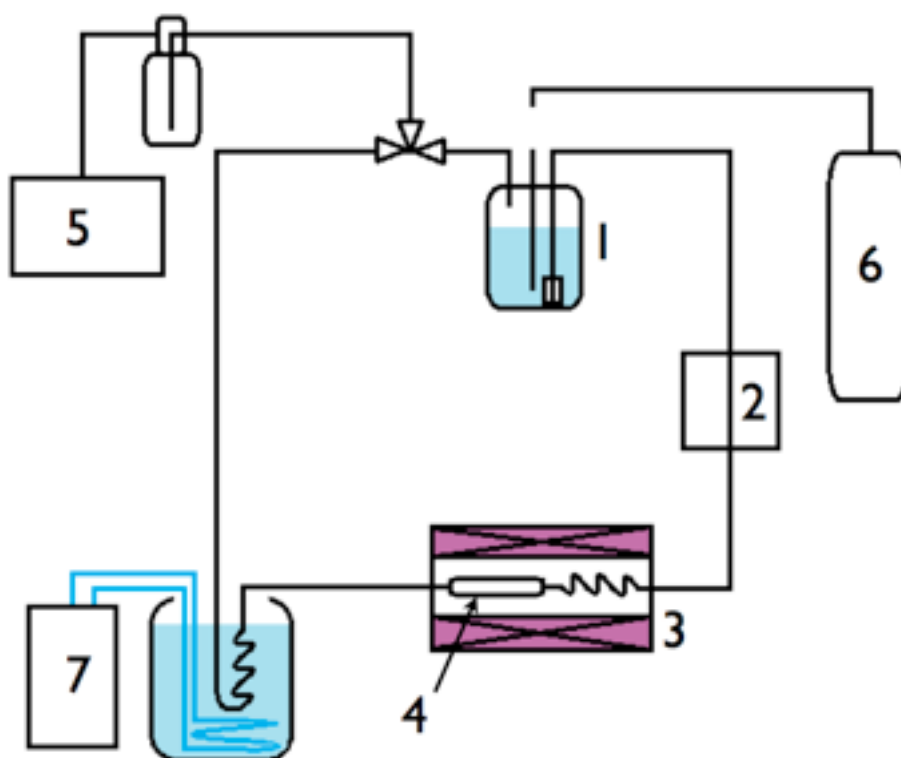
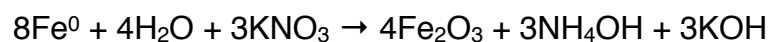
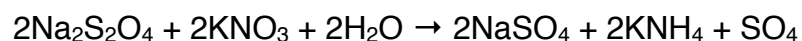


Figure 1: Continuous flow catalysis. 1: Stock solution, 2: liquid chromatography pump, 3: Cylindrical furnace, 4: filter holder, 5: vacuum pump, 6: N₂ gas, 7: water cooler.

In the use of sodium dithionite & nitrate as well as nitrate & solid iron the production of ammonia is expected from the following equations:



However, the production of ammonia from solid iron and N₂ is not expected to be seen without the presence of a zeolite as the kinetic energies provided does not spontaneously reduce N₂ (Table 2).

Table 2: Potentials of elements and their compounds at 25°C (Dean 1999).

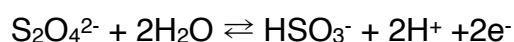
Reaction	Standard or formal potential
$\text{Fe}^{3+} + \text{e}^- \rightleftharpoons \text{Fe}^{2+}$	0.771
$\text{Fe}^{2+} + 2\text{e}^- \rightleftharpoons \text{Fe}^0$	-0.44
$\text{N}_2 + 2\text{H}_2\text{O} + 4\text{H}^+ + 2\text{e}^- \rightleftharpoons 2\text{HONH}^+$	-1.87
$\text{N}_2\text{O} + 6\text{H}^+ + \text{H}_2\text{O} + 4\text{e}^- \rightleftharpoons 2\text{HONH}_3^+$	-0.05
$2\text{NO} + 2\text{H}^+ + 2\text{e}^- \rightleftharpoons \text{N}_2\text{O} + \text{H}_2\text{O}$	1.59
$\text{HNO}_2 + \text{H}^+ + \text{e}^- \rightleftharpoons \text{NO} + \text{H}_2\text{O}$	0.996
$\text{NO}_3^- + 3\text{H}^+ + 2\text{e}^- \rightleftharpoons \text{HNO}_2 + \text{H}_2\text{O}$	0.94

Samples of the reacted solution were taken at the end of the catalysis and divided into preparation for the analysis of ammonia and carbon. The vials used for analysis of ammonia, were vacuumed before injecting with 5 ml sample and 20 μl dichloromethane to prevent bacteria growing. The pin hole is then covered by nail polish to ensure it is sealed. Samples for analysis of carbon were stored in fridge in the case they could not be treated immediately. While all samples for analysis of ammonia were stored in fridge with vacuum seal until analysis.

Ammonia analysis

Concentrations of N in the form of ammonium were determined using a method based on Solórzano (1969). This method use spectrophotometry (Techicon TM Autoanalyser II, S.C. Colorimeter), measuring the blue colour of nitrosobenzene. Nitrosobenzene is formed at high pH. through diazotization of phenol and oxidation of the diazo compound using sodium hypochlorite (NaClO).

Some issues of sample analysis occurred, due to the redox potential of $\text{Na}_2\text{S}_2\text{O}_4$ (Mayhew 1978). Whereby the reducing compound has the potential to negate the oxidising solution through redox (below equation), preventing nitrosobenzene to be formed, maintaining a clear solution.



This effect was negated by adding oxalic acid, to oxidise the SDT still in solution. The analysis may however have given lower concentrations than there should be.

C-compounds

The catalytic solutions were investigated for low number C-chains (C_{1-8}) to distinguish whether there was any contamination or not, using GCMS. A Shimadzu GCMS-QP2010 Ultra, with FID, AOC20i auto injector and deans switching device was used with a Varian CP-PoraBOND Q, fused silica column (50 m long x 0.32 mm Internal diameter). The program temperature at first isothermal at 50°C for 4 min and heated to 150°C using a rate of 10°C min^{-1} . This was followed by a second heating to 150°C with 15°C min^{-1} and kept isothermal for 9.33 min. Helium was used as a carrier gas at a 3.5 ml min^{-1} rate. The gas chromatograph was interfaced at 150°C into the QP2010 Ultra quadropole mass spectrometer. The mass analyser operated in full scan mode from 20-50 m/z using

electron impact at 70 eV with a resolution of 1 m/z. The ionisation chamber and quadropole was set to 250°C and 100°C respectively. Each compound was characterised by its mass fragment pattern and compared with the NIST 2010 spectra library.

The samples of solution from catalysis were mixed with 50 ml of dichloromethane and placed in ultra sonic bath for 3-5 min and then concentrated using a rotating evaporator. The calibration curve was done using 10^{-3} , 10^{-4} , 10^{-5} , 10^{-6} mol l⁻¹ of pyridine in dichloromethane.

Statistics

Statistics were conducted using SPSS v.21.

Due to the small sample size, and homogeneity of variance showing to reject null hypothesis (H_0 = variance within groups are normally distributed), the non-parametric Kruskal-Wallis test was conducted (Similar to 1-way ANOVA) and the non-parametric post-hoc test Dunnett T3 pairwise comparison, was conducted to distinguish significance between groups.

Non-parametric tests (when assumptions are met) have little chance of making a type 1 error (rejecting the null hypothesis, when it is true) It is however a greater chance of making a type 2 error, retaining the H_0 hypothesis when it is false. There is therefore a chance to see more significance than is really there! The Dunnett T3 test was chosen as the T3 is more suitable for small sample sizes.

Results

ESEM

Multiple measurements of elemental analysis using EDS gave relative proportions of elements that were used to give ratios of the crystalline product (Table 3) to characterise the product achieved. A Levene's test of homogeneity of variance showed that the variance between synthesised products are not equal for Si/Al ($F = (8, 51) 5.752$, $p < 0.05$) and Fe/Si ($F = (8, 51) 4.746$, $p < 0.05$). A Kruskal-Wallis test show there is a significant difference ($p < 0.05$) at $\alpha = 0.05$ for both Si/Al and Fe/Si ratios between all products. The

Dunnnett T3 post hoc test (Appendix 1.1) show that products 1-3 and 4, 5 are the same crystals based on the Si/Al ratios. It also show that products 7, 8 & 9 are all different crystals. Finally the Fe/Si ratios indicate the incorporation of iron *in situ* of the synthesis was successful for all three zeolites.

Table 3: Ratios of products and *in situ* syntheses products. Temperature and reaction time.

Reaction #	Si / Al	(K + Na) / Si	Fe / Si	Fe / (K + Na)	Temp °C	Time h
Phillipsite						
1	1.91	0.65	0	0	140	72
2	1.82	0.65	0.10	0.16	140	72
3	1.86	0.61	0.21	0.34	140	72
Analcime						
4	3.24	0.23	0	0	200	24
5	1.71	0.67	0.15	0.22	150	72
6	1.88	0.64	0.15	0.24	150	72
Clinoptilolite / Sanidine						
7	3.20	0.65	0	0	195	37
8	3.38	0.51	0.08	0.15	195	72
9	2.48	0.63	0.12	0.18	195	72

Levene's test also show that there are significant differences in the variance of Si/Al and Fe/Si respectively for post-synthesis iron incorporation for product #1 ($F = (5, 36) 19.691$, $p < 0.05$ & $F = (5, 36) 12.493$, $p < 0.05$), product #4 ($F = (5, 36) 8.889$, $p < 0.05$ & $F = (5, 36) 2.495$, $p < 0.05$), and product #7 ($F = (5, 35) 5.749$, $p < 0.05$ & $F = (5, 35) 10.642$, $p < 0.05$). A Kruskal-Wallis test does not show a significant difference for Si/Al ratios ($p > 0.05$, $\alpha = 0.05$) between treatments of phillipsite, while Fe/Si does ($p < 0.05$, $\alpha = 0.05$). The treatments of analcime are significantly different for both Si/Al ($p < 0.05$, $\alpha = 0.05$), and Fe/Si ($p < 0.05$, $\alpha = 0.05$). For the treatments of clinoptilolite / sanidine there is no significant difference in Si/Al ($p > 0.05$, $\alpha = 0.05$), while the Fe/Si is significantly different ($p < 0.05$, $\alpha = 0.05$). The Si/Al and Fe/Si ratios of treated products (Table 4) were also compared using the post doc test Dunnnett T3 in appendix 1.2, 1.3 and 1.4 for phillipsite, analcime and clinoptilolite/sanidine respectively and their iron *in situ* syntheses.

The results from the post hoc test show that the Si/Al and Fe/Si ratios are significantly different between the groups of synthetic products, indicating they are different types of

zeolites. A Dunnett T3 post hoc test show the Si/Al ratio does not change significantly with treatment of phillipsite, meaning the treatments do not change the crystallography of the sample, while the incorporation of Fe into the structure post synthesis was only successful with the ammonium bicarbonate and iron treatment. In the case of analcime, the crystallography is affected when comparing the Si/Al ratios between treatments, it does however also show a successful incorporation of iron post-synthesis. The treatments of sanidine has a similar story to phillipsite, where the Si/Al ratios does not change with treatments, keeping the crystal structure intact; however, there was no significant incorporation of iron into the structure of sanidine.

Table 4: Ratio of elements from elemental analysis. Showing product from reaction 1, 4 and 7, with their 3 modifications, and the ammonium bicarbonate and nitric acid intermediary steps.

Post-synthesis treatment	Si / Al	(K + Na) / Si	Fe / Si	Fe / (K + Na)
1: Fe	1.71	0.64	0.03	0.05
1: NH ₄ HCO ₃ + Fe	1.67	0.56	0.03	0.05
1: HNO ₃ + Fe	276.90	0.01	0.01	0.92
1: NH ₄ HCO ₃	1.82	0.61	0	0
1: HNO ₃	150.67	0.05	0	0
4: Fe	3.32	0.32	0.42	1.30
4: NH ₄ HCO ₃ + Fe	3.84	0.27	0.02	0.06
4: HNO ₃ + Fe	3.40	0.28	0.00	0.00
4: NH ₄ HCO ₃	3.09	0.27	0	0
4: HNO ₃	3	0.28	0	0
7: Fe	3.27	0.41	0.01	0.03
7: NH ₄ HCO ₃ + Fe	3.36	0.49	0.02	0.04
7: HNO ₃ + Fe	3.33	0.45	0.01	0.03
7: NH ₄ HCO ₃	3.35	0.50	0	0
7: HNO ₃	3.48	0.54	0	0

In Fig 2, the samples are seen to be homogenous for all syntheses except for #8 and 9, where both contain two crystal phases. For product #1-3, the crystals have a twinning pattern, growing in 3-dimensional cross like stars. For product #4, the crystals are spherical, while its *in situ* iron counter parts, #5 & #6 have a rod like crystal shape as. For product # 7 the crystals have a flat, flakey appearance, while its iron counterparts #8 has a mix of the platy crystals with rod like crystals such as #5 & #6, while #9 has no platy crystals but rather rod like and dog bone like crystals.

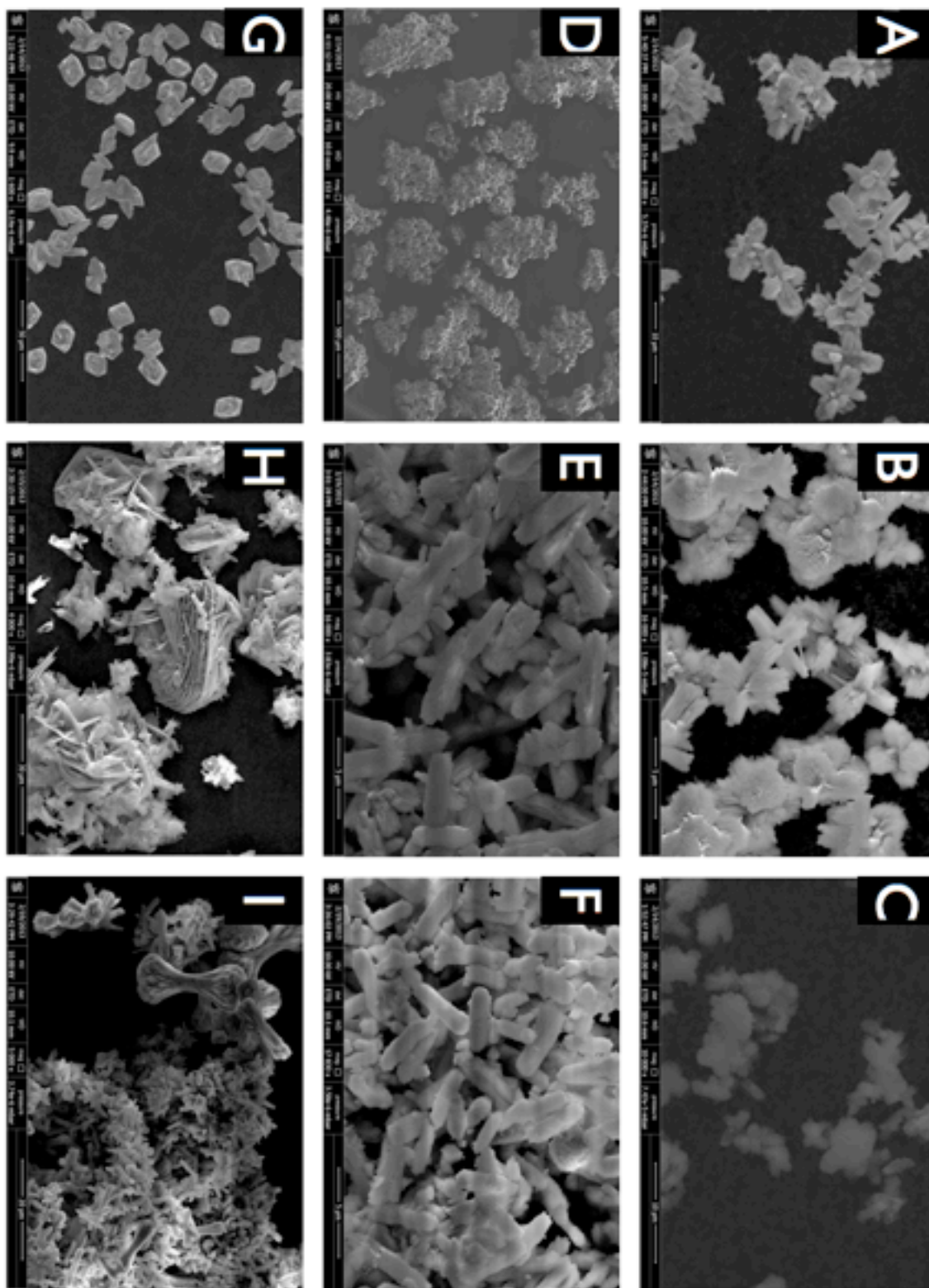


Figure 2: Products from reaction mixtures (Table 3) viewed in ESEM, a) 1, b) 2, c) 3, d) 4, e) 5, f) 6, g) 7, h) 8, i) 9.

PXRD

X-ray diffraction analysis show that the synthesized products do not maintain the same crystallography when they are synthesized with iron *in situ* (Table 5). Products 1-3 and 4-5 coincide with the reference to phillipsite. Meaning the samples have the same crystallography. The #4 synthesis coincides with analcime while products #7-9 coincide with sanidine, a felspar rather than zeolite. The #9 synthesis however only coincide with feldspar at a low level and match the crystallography of merlinoite to 65.6%. These differences are more clearly seen in appendix 2.1 for phillipsite, appendix 2.3 for analcime, and appendix 2.5 for sanidine. With the respective peak values in appendix 2.2, 2.4 & 2.6. The crystallographic information of synthesized products can be seen in table 6. The unit cell volume given represent the pattern of increase/decrease seen later in the BET analysis for phillipsite and sanidine surface area. The unit cell volume for analcime however does not show the same pattern, and the values calculated are not of those expected as analcime is cubic and should have three equally large values for bonding distance.

Table 5: % of crystallinity of the spectra overlapping with the reference. Product number of the synthesis is shown in square brackets. The phases detected were: 1) Phillipsite (Galli & Ghittoni 1972), 2) Analcime (Taylor 1930), 3) Sanidine (Keefer & Brown 1978) and 4) Merlinoite (Passaglia *et al.* 1977).

	% of Crystallinity (Other phases)		
	Phillipsite ¹	Analcime ²	Sanidine ³
Synthetic	67.1 [1]	80.9 [4]	93.4 [7]
Zeolite Fe (II)	71.2 [2]	0 (58 ¹) [5]	85.5 [8]
Zeolite Fe (III)	65.8 [3]	0 (61 ¹) [6]	>5 (65.6 ⁴) [9]

Table 6: Crystallographic information of samples and references 1) Chen *et al.* 2002 , 2) Joshi *et al.* 1983 ,3) Woensdregt 1983,4) Passaglia *et al.* 1977

	a (Å)	b (Å)	c (Å)	α	β	γ	Crystal Symmetry	Unit cell-Volume (Å ³)
Phillipsite reference ¹	10.01	14.28	14.21	90	90	90	Orthorhombic	2032
Phillipsite	12.76	10.22	9.94	90	90	90	Orthorhombic	1298
Phillipsite Fe II	15.50	10.50	7.12	90	90	90	Orthorhombic	1160
Phillipsite Fe III	14.37	9.94	7.11	90	90	90	Orthorhombic	1411
Analcime reference ²	13.71	13.71	13.71	90	90	90	Cubic	2581
Analcime	13.36	13.36	13.36	90	90	90	Cubic	2385
Analcime Fe II	21.48	15.10	6.60	90	90	90	Orthorhombic	2142
Analcime Fe III	28.50	8.13	6.41	90	90	90	Orthorhombic	1487
Sanidine reference ³	8.5602	13.03	7.19	90	115.99	90	Monoclinic	720
Sanidine	7.17	14.84	9.23	26.67	124.90	118.83	Triclinic	360
Sanidine Fe II	8.37	9.24	15.63	131.09	69.17	127.84	Triclinic	727.39
Sanidine Fe III	14.14	14.11	9.96	90	90	90	Orthorhombic	1988
Merlinoite reference ⁴	14.11	14.22	9.94	90	90	90	Orthorhombic	1994

FT-IR

The infra red spectra of dry sample with pyridine, in this case a deconvolution spectra from phillipsite (figure 3) show an apparent broadening and deepening of the peak of the sample. The peak is also showing a slight shift to the left. This broadening and shift of the peak indicate that there are Brønsted acid sites. Meaning that the crystals has the ability to bond to N_2 . The IR spectra show a good correlation for phillipsite (Appendix 3.1.1) while there are some differences of analcime (Appendix 3.2.1) and sanidine (Appendix 3.3.1). The broadening of the peak is seen in the *in situ* synthesis for Phillipsite (Appendix 3.1.2), analcime (Appendix 3.2.2) and sanidine (Appendix 3.3.2). Broadening of the peaks are also seen when de-aluminising the crystals and introducing the iron post-synthesis. This can be seen for Phillipsite (Appendix 3.1.3), Analcime (Appendix 3.2.3) and Sanidine (Appendix 3.3.3). The peaks seen around 3500 cm^{-1} can be explained by the physical adsorption onto the surface area due to an extensive formation of hydrogen bonds with iron oxo- and hydroxo-species (Doula 2007). The peaks seen at $\sim 2900\text{ cm}^{-1}$ is a contamination from the sample preparation that is also seen in when running blanks and the peaks around 2300 cm^{-1} are those of CO_2 from the air, used to vent the system. The remaining peaks in all samples coincide with those of other zeolites where remaining water in the crystal structure is seen $\sim 1650\text{ cm}^{-1}$. The peaks around $900\text{-}1100\text{ cm}^{-1}$ represent the stretching of Al-Si in particular and those at 780 cm^{-1} and lower are mainly Si-O stretching. For full details see appendix 3.4.

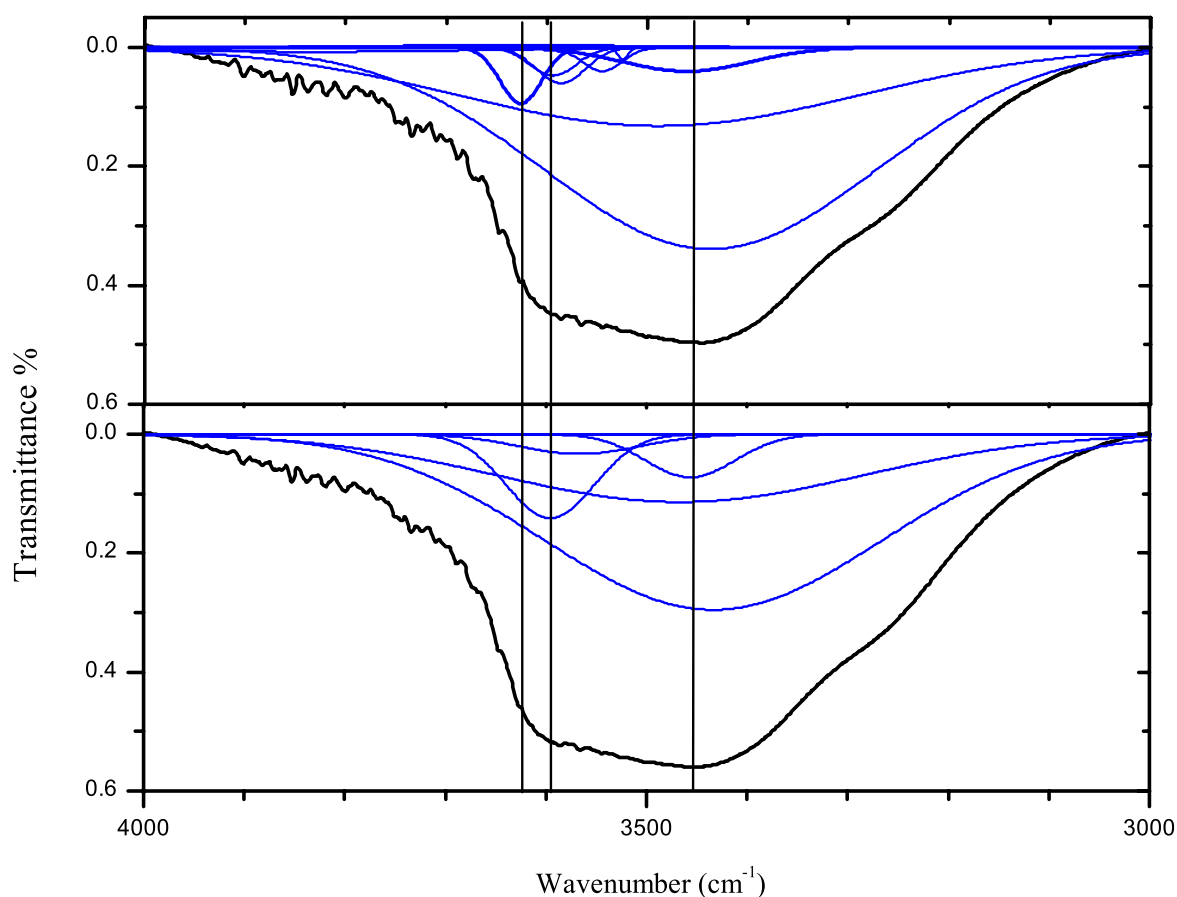


Figure 3: Peak deconvolution with gaussian peaks of Phillipsite (on top) and Phillipsite with pyridine (bottom). The black line represent the peak observed in FTIR, blue lines represent deconvoluted peaks from the original spectra.

BET

Surface area analysis further show that the samples of sanidine and analcime are similar to those reported in reference while the synthesised phillipsite has a much larger surface area than its reference (Figure 4). It is also seen as a general trend that the surface area increases when iron is included in the framework. For Sanidine and analcime it is seen that the surface area with Fe^{2+} and Fe^{3+} in synthesis both increase the surface area. For Phillipsite it shows that the surface area drops somewhat when synthesised with Fe^{2+} while Fe^{3+} increases the surface area. This pattern is also seen for pore volume (Appendix 4.1) of the crystals and pore surface area (Appendix 4.2). Pore diameter however (appendix 4.3) is the largest for Analcime, while it is relatively unchanged for all samples except sanidine Fe II that has a slightly higher peak.

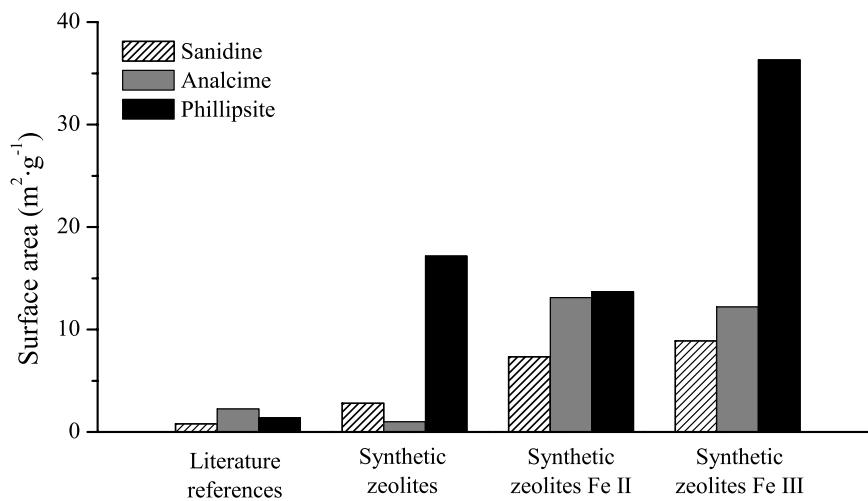


Figure 4: Surface area of samples with literature references for synthetic phillipsite (Cichocki *et al.* 1979), analcime (Line *et al.* 1995) and sanidine (Hodson 1999).

Catalysis

N-analysis

A calibration curve was done for ammonia analysis seen in Fig 5, showing a good fit and was thus used to derive the ammonia values for the samples.

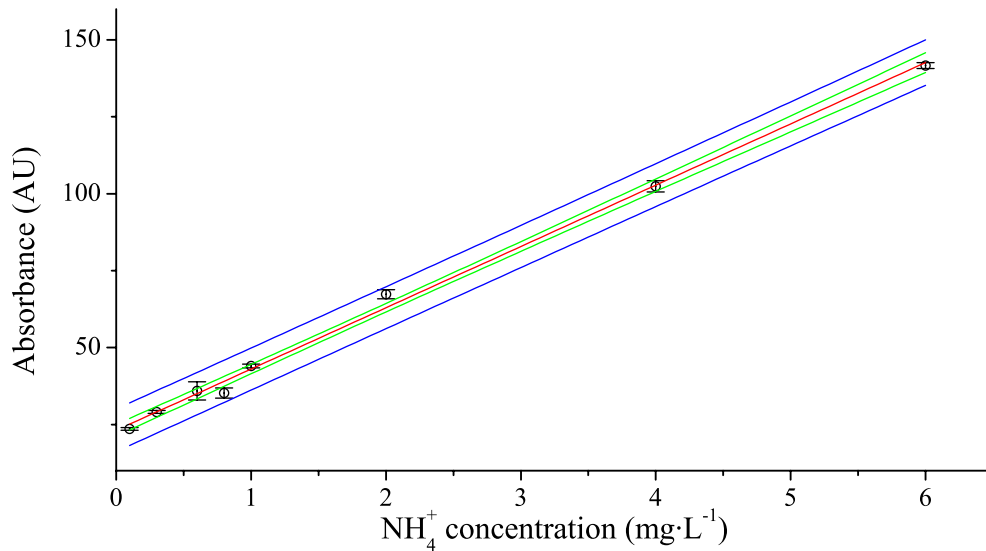


Figure 5: Calibration curve NH₄⁺ analysis (linear fit), $R^2 = 0.99$, and 95% confidence intervals.

The production of ammonia can be seen in table 7, showing a generally low rate of ammonia production around 1-3 mg NH₄⁺ m⁻² g⁻¹ day⁻¹ for Phillipsite and its iron counterparts. The production rate for analcime iron counterparts is also low, around 1.82-3.56 mg NH₄⁺ m⁻² g⁻¹ day⁻¹. For Analcime by itself the production rate of ammonia is rather high, at 26.63-34.66 mg NH₄⁺ m⁻² g⁻² day⁻¹. Giving analcime the highest rate of NH₄⁺ production by approximately one magnitude more than the other samples.

Table 7: Samples in catalytic reactions. The abbreviations are:FC = Flow catalysis; SDT = Sodium Dithionite; IC = Iron chips; IP = Iron powder.

Crystal	Catalysis	SDT	KNO ₃	Fe-Source	N ₂	pre-pH	post-pH	% Conversion of N-source	Rate mg NH ₄ m ⁻² g ⁻¹ day ⁻¹
Ana	FC	X	X	-	-	10	3	29.80	26.63
Ana	AC	-	X	IC	-	10	9	38.19	34.12
Ana	AC	-	-	IC	X	10	9	38.79	34.66
Ana Fe II	FC	X	X	-	-	10	5	26.53	1.82
Ana Fe II	AC	X	X	-	-	10	4.5	31.36	2.16
Ana Fe II	AC	-	X	IC	-	10	6	30.09	2.22
Ana Fe II	AC	-	-	IC	X	10	7	51.80	3.56
Ana Fe III	FC	X	X	-	-	10	4.5	31.01	2.69
Ana Fe III	AC	-	X	IC	-	10	5	33.74	2.77
Ana Fe III	FC	-	-	IP	X	10	6	38.14	3.13
Ana Fe III	AC	-	-	IC	X	10	7	36.92	2.72
Phi	AC	-	X	IC	-	10	13	39.10	2.05
Phi	AC	-	-	IC	X	10	9	38.36	2.01
Phi Fe II	FC	X	X	-	-	10	-	34.16	2.25
Phi Fe II	AC	-	X	IC	-	10	9	42.76	2.81
Phi Fe II	AC	-	-	IC	X	10	13	38.57	2.54
Phi Fe III	FC	X	X	-	-	10	-	46.83	1.16
Phi Fe III	FC	X	X	-	-	10	-	32.08	0.80
Phi Fe III	AC	X	X	-	-	10	-	64.72	1.61
Phi Fe III	AC	-	X	IC	-	10	13	52.81	1.31
Phi Fe III	FC	-	-	IC	X	10	9	38.68	0.96
Phi Fe III	AC	-	-	IC	X	10	7	40.58	1.01

C-Analysis

GCMS analysis revealed that most samples had produced 3-Methyl-2-Butanone, less than 10⁻⁴ M, indicating there was a small CO₂ contamination in the process. This should however have little effect on the production of NH₄, the purpose of this catalysis.

Discussion

The zeolites intended for synthesis were phillipsite, analcime and clinoptilolite by using reaction mixture ratios from references with successful synthesis of each desired mineral. As it turned out, phillipsite was the only mineral in this study, to successfully maintain its crystallography when iron was added *in situ*. As for analcime, both Fe²⁺ and Fe³⁺ resulted in the crystallography phillipsite phillipsite, though visually, the crystals were not twinned but had a fibrous appearance such as phillipsite in ESEM. The reaction mixtures for clinoptilolite turned out to produce sanidine in flat and stacked crystals. When introduced to Fe²⁺ and Fe³⁺, another sanidine and merlinoite were produced, respectively. Sanidine is not an unlikely candidate in the synthesis of clinoptilolite, as it has been reported before (Satokawa & Itabashi 1997). When looking at the Si/Al ratio, merlinoite does have a different ratio, however the reason this crystal was produced is unknown, the synthesis of clinoptilolite has shown other products than that intended, e.g. phillipsite, sanidine and

mordenite (Satokawa & Itabashi 1997). The incorporation of iron post-synthesis was also successful, though the amount of iron is less than that introduced *in situ*. Analcime (product 4) has a high content of iron, when compared in its Fe/Si ratio. The PXRD analysis show a high match of the products with its references, however not all do. In particular the phillipsite products and the Fe²⁺ analcime and Fe³⁺ zeolites of analcime and sanidine. This indicated that there could be an interaction with a crystal structure not seen. As for the Brønsted acid sites, all products, with and without iron synthesis *in situ* showed the presence of acid sites when pyridine was added through broadening of the peaks. This was also seen for post-synthesis treatments for all products, indicating that acid sites can be created by de-aluminising the crystals. The BET surface analysis revealed a general trend in the increase of both surface, pore volume and pore surface area. Indicating that the presence of iron in a solution can not only change the characteristics of a crystal by having iron centres that can enable catalytic reactions. But also changes the physical structure of the crystals. As the mineral surface of zeolites themselves can induce reactions and the structure of the zeolite act as a source or sink for prebiotic chemistry (Schoonen *et al.* 2004). The inclusion of iron may increase the catalytic potential of the mineral. The BET also revealed that analcime had the largest pore diameter. This will affect the absorptive characteristics between the products. As a larger pore diameter may increase the amount of molecules that can enter the crystal frame and what types of molecules that fit. Even though the pore volume for analcime is relatively small, the pore diameter could potentially enhance the catalysis as well.

Due to time constraint only the two zeolites phillipsite and analcime was used for the catalytic experiments, as these are expected to have the greatest catalytic ability of the three products synthesised. The catalysis was divided into two sets. One was a continuous flow system where the solution was pushed through a filter holding the zeolites. The other was using the teflon lined autoclaves used for the synthesis of the products. This catalysis is expected to be more harsh on the crystals, and one cannot say for certain where the reaction occurs in the solution. As well as the risk for contamination from the autoclave teflon and a small risk of the solution reacting with the steel of the container holding the teflon liner. The analysis of NH₄⁺ ions was troublesome in terms of reacting with the oxidising reagents of the NH₄⁺ analysis. This was corrected with oxalic acid; however, the values given could still be an underestimation of the real values. Even so, NH₄⁺ was produced in both the continuous flow system and in the autoclaves. Upon initial inspection of the production rates there does not seem to be a noticeable difference in NH₄⁺ production between the two systems. There is also no obvious pattern in NH₄⁺ production based on the components used, e.g. NO₃⁻ vs. N₂, and the reducing agents, solid iron vs. sodium dithionite. Although phillipsite may be expected to have the greatest catalytic ability due to its high surface area and fibrous looks, the product that yielded the highest rate was analcime. The NH₄⁺ production rate with analcime was a magnitude (10 times) higher than that of the rest of the crystals. Considering that the crystallography tells us all other samples are phillipsite, the small differences between these are not surprising. Analcime however had the smallest surface area and the biggest pore diameter. It produced as much as 26.84 mg NH₄⁺ m⁻² g⁻¹ day⁻¹ in the continuous flow system with SDT and KNO₃. In the autoclave catalysis, analcime had rates of 34.4 mg NH₄⁺ m⁻² g⁻¹ day⁻¹ and 34.94 mg NH₄⁺ m⁻² g⁻¹ day⁻¹ using KNO₃ & solid iron and solid iron & N₂ respectively. Showing that analcime produced the highest rates in all combinations of N-source and reducing agents used in this study. Compared to previous studies the reduction of N₂ into NH₄⁺ has been seen at temperatures of 300-800°C and conversion rates of 17% at 700°C and 0.1 GPa, imitating lithospheric settings (Brandes *et al.* 1998). Another synthesis from air, using electrical currents has been seen at rates of 0.04219 mg m⁻² day⁻¹. (Lan *et al.* 2013).

This shows that not only is the conversion rate a lot higher in this study using zeolites as catalysts, but the conversion rate of up to 64% is also higher than what has been previously found. Even though N-reduction in the presence of metallic iron has been seen, the study gave higher values at high temperatures of 200°C with rates of 187 $\mu\text{mol NH}_4^+$ $\text{kg}^{-1} \text{Fe}^0$ used (Smirnov et al 2008). As 200°C is considered too high for the formation of life, and the blanks of this study using Argon, produced ammonia, the contamination rate in the study can be discussed.

Also to note is the post-synthesis pH of the reaction solution, where the most acidic solution gives the lowest rates and the highest pH gave the highest production rate. This may be worth investigating as the efficiency of the reducing agents would change with the pH. It needs to be taken into consideration however, that many of the solutions where SDT was used, end-pH was lower. Indicating that the low pH may be due to the formation of sulphuric acid from STD oxidation. It was also found that the catalytic solution contained some C-contamination, unfortunately due to the lack of proper internal references the values can not be properly estimated are thus not included in this report but it is estimated to be less than 10^{-4} M if it is compared to the calibration curve for N-compounds. This could be either from the handling of samples or a CO_2 adsorbed or small leak in the catalytic systems. It should however not have any major impact on the NH_4 production even in the case microorganisms may have been able to enter the system as the pH and the temperature of the reactions should have defended against most of the microbes.

Future aspects from this study is to continue the synthesis of other zeolites and investigate the catalytic efficiency using the continuous flow system to confidently estimate the production rate of ammonia from the crystals. The neutralisation of SDT is also required to be further investigated to acquire the correct production rates of NH_4

The take home messages from this study are:

- The crystallography of phillipsite, analcime and sanidine are affected by the presence of both Fe^{2+} and Fe^{3+} in solution during synthesis. This increases the surface area, pore volume and pore surface area. Pore diameter however did not show to change with the addition of iron.
- The catalysis does generate NH_4^+ in both a continuous flow system and a non-site specific autoclave system. Pore diameter or the number of Brønstedt acid sites may be an important factor as the rate of NH_4^+ produced was a magnitude higher for all analcime catalytic reactions. As the production of NH_4^+ is not energetically favourable when solutions are used by themselves, the fact that NH_4^+ was produced here, does indicate that zeolites may have had an important role in the production of NH_4^+ for prebiotic chemistry.
- The ability of N-fixation, using two commonly found zeolites, can be extended to other zeolitic minerals formed in hydrothermal systems, and should be investigated.
- These results indicate that shallow /low pressure environments at ambient temperatures of $\sim 100^\circ\text{C}$ likely have the capability of N-fixation. This can be done with not only NO_3^- , but also from N_2 in alkaline conditions of pH 10. Giving the N-source needed for the prebiotic chemistry of molecules such as amino-acids that has been shown to be produced in the presence of N and CO (Rao *et al.* 1980).

References

- Anbalagan G., Sankari G., Ponnusamy S., Kumar R.T. & Gunasekaran S. (2009) Investigation of silicate mineral sanidine by vibrational and NMR spectroscopic methods. *Spectrochimica Acta Part A: Molecular and Biomolecular Spectroscopy*. 74 (2): 404–409.
- Ates A. & Hardacre C. (2012). The effect of various treatment conditions on natural zeolites: Ion exchange, acidic, thermal and steam treatments. *Journal of Chromatography A*. 372 (1): 130–140.
- Barrett E.P., Joyner L.G., & Halenda P.P. (1951) The determination of pore volume and area distributions in porous substances. I. Computations from nitrogen isotherms. *Journal of the American Chemical Society*. 73 (1): 373–380.
- Brandes J.A., Boctor N.Z., Cody G.D., Cooper B.A., Hazen R.M. & Yoder Jr H.S. (1998) Abiotic nitrogen reduction on the early earth. *Nature*. 395: 365-367.
- Brunauer S., Emmett P.H. & Teller E. (1938) Adsorption of gases in multimolecular layers. *Journal of the American Chemical Society*. 60: 309-319.
- Chen H-F., Lo H-J., Song S-R., Fang J-N., Chen Y-L., Li L-J., Lin-I-C., Chung S-H. & Lee Y.T. (2002) The synthesis of phillipsite. *Western pacific earth sciences*. 2 (4): 381-392.
- Cichocki A., Grochowski J. & Lebioda Ł. (1979) Phillipsite-type synthetic zeolite with high silica contents and accompanying phases. *Kristall und technik*. 14 (1): 9-18.
- Csicsery S.M (1984) Shape-selective catalysis in zeolites. *Zeolites*. 4 (3): 202-213.
- Dean J.A. (1999) Lange's handbook of chemistry. 1174-1343. 15th Ed. *McGraw-Hill*. New York.
- Doula M.K. (2007) Synthesis of a clinoptilolite-Fe system with high Cu sorption capacity. *Chemosphere*. 67: 731-740.
- Dzwigaj S. Massiani P. Davidson A. & Che M. (2000) Role of silanol groups in the incorporation of V in β zeolite. *Journal of molecular catalysis A: Chemical*. 155: 169-182.
- Galli E. & Ghittoni A.G.L. (1972) The crystal chemistry of phillipsites. *American Mineralogist*. 57: 1125-1145.
- Goldsmith J. R. & Laves F. (1954) The microcline-sanidine stability relations. *Geochimica et Cosmochimica Acta*. 5 (1): 1–19.
- Hendrich M.P., Gunderson W., Behan R.K., Green M.T., Mehn M.P., Betley T.A., Lu C.C. & Peters J.C. (2006) On the feasibility of N₂ fixation via a single-site Fe^I/Fe^{IV} cycle: spectroscopic studies of Fe^I(N₂)Fe^I, Fe^{IV}=N, and related species. *PNAS*. 103 (46): 17107-17112.
- Hodson M.E. (1999) Micropore surface area variation with grain size in unweathered alkali feldspars: Implications for surface roughness and dissolution studies. *Geochimica et cosmochimica acta*. 62 (21/22): 3429-3435.

Javoy M. (2005) Where do the oceans come from?. *Comptes Rendus Geoscience*. 337 (1): 139-158.

Joshi M. S., Choudhari A. L., & Kanitkar R. (1983) Synthesis of analcime-type zeolite from natural stilbite by hydrothermal method. *Crystal Research and Technology*. 18 (11): 1347–1351.

Keefer K. D. & Brown G. E. (1978) Crystal structures and compositions of sanidine and high albite in cryptoperthitic intergrowth. *American Mineralogist*. 63 (11-12): 1264–1273.

Kesraoui-Ouki S., Cheeseman C.R. & Perry R. (1994) *Journal of chemical technology and biotechnology*. 59: 121-126.

Kim D., & Chung H. (2003) Synthesis and characterization of ZSM-5 zeolite from serpentine. *Clay minerals and the environment*. 24: 69–77.

Lan R., Irvine J.T.S. & Tao S. (2013) Synthesis of ammonia directly from air and water at ambient temperature and pressure. *Scientific reports*. 3: 1145.

Line C.M.B., Putnis A., Putnis C. & Giampaolo C. (1995) The dehydration kinetics and microtexture of analcime from two parageneses. *American mineralogist*. 80: 268-279.

Martin W., Baross J., Kelley D. & Russell M.J. (2008) Hydrothermal vents and the origin of life. *Nature reviews. Microbiology*. 6: 805-814.

Mayhew S.G. (1978) The redox potential of dithionite and SO₂- from equilibrium reactions with flavodoxins, Methyl Viologen and hydrogen plus hydrogenase. *European journal of biochemistry*. 85 (2): 535-547.

Ming D.W. & Boettinger J.L. (2001) Zeolites in soil environments. In: Geology, Mineralogy, Properties, and utilization of natural zeolites. Ed: Bish D.L. and Ming D.W.. Reviews in mineralogy and geochemistry. *Mineralogical society of America*.

Nitschke W. & Russell M.J. (2009) Hydrothermal focusing of chemical and chemiosmotic energy, Supported by delivery of catalytic Fe, Ni, Mo/W, Co, S and Se, forced life to emerge. *Journal of molecular evolution*. 69: 481-496.

Passaglia E., Pongiluppi D. & Rinaldi R. (1977) Merlinoite, a new mineral of the zeolite group. *Neues Jahrbuch für mineralogie - monatshefte*. 01: 355-364.

Rao M., Odom D.G. & Oró J. (1980) Clays in prebiological chemistry. *Journal of molecular evolution*. 15: 317-331.

Ríos C.A. & Williams C.D. (2008) Synthesis of zeolitic materials from natural clinker: a new alternative for recycling coal combustion by-products. *Fuel*. 87: 2482-2492.

Rodriguez M.M., Bill E., Brennessel W.W. & Holland P.L. (2011) N₂ Reduction and hydrogenation to ammonia by a molecular iron-potassium complex. *Science*. 334: 780-783.

Rouquerol J., Avnir D., Fairbridge C.W., Everett D.H., Haynes J.H., Pernicone N., Ramsay J.D.F., Sing K.S.W. & Unger K.K. (1994) Recommendations for the characterization of porous solids. *Pure and applied chemistry*. 66 (8): 1739-1758. (© 1994 IUPAC). p

Satokawa S. & Itabashi K. (1997) Crystallization of single phase (K, Na)-clinoptilolite. *Microporous materials*. 8: 49-55.

Schoonen M., Smirnov A. & Cohn C. (2004) A perspective on the role of minerals in prebiotic systems. *Ambio*. 33 (8): 539-551.

Singireddi S., Gordon A.D., Smirnov A., Vance M.A., Schoonen M.A.A. Szilagyi R.K. & Strongin D.R. (2012) Reduction of nitrite and nitrate to ammonium on pyrite. *Origins of life and evolution of the biosphere*. 42 (4): 275-294.

Smirnov A., Hausner D., Laffers R., Strongin D.R. & Schoonen M.A.A. (2008) Abiotic ammonium formation in the presence of Ni-Fe metal and alloys and its implications for the Hadean nitrogen cycle. *Geochemical transactions*. 9: 5.

Solórzano L. (1969) Determination of ammonia in natural waters by the phenylhypochlorite method. *Limnology and oceanography*. 14 (5): 799-801.

Stüeken E.E., Anderson R.E., Bowman J.S., Brazelton W.J., Colangelo-Lillis J., Goldman A.D. Som S.M. & Baross J.A. (2013) Did life originate from a chemical reactor?. *Geobiology*. 11: 101-126.

Summers D.P. (1999) Sources and sinks for ammonia and nitrite on the early earth and the reaction of nitrite with ammonia. *Origins of life and evolution of the biosphere*. 29: 33-46.

Tatlier M., Cigizoglu K.B., Tokay B., & Erdem-Şenatalar A. (2007) Microwave vs. conventional synthesis of analcime from clear solutions. *Journal of crystal growth*. 306: 146-151.

Taylor W H (1930) I. The structure of analcite ($\text{NaAlSi}_2\text{O}_6 \cdot \text{H}_2\text{O}$). *Zeitschrift für Kristallographie*. 74: 1-19.

Taylor S.R. & McLennan S.M. (2009) The hadean crust of the earth. 233-248. In: Planetary crusts: their composition, origin and evolution. *Cambridge University press*. Cambridge, UK.

Trail D., Watson B.A. & Tailby N.D. (2013) Insights into the Hadean earth from experimental studies of zircon. *Journal of geological society of india*. 81: 605-636.

Weitkamp J. (2000) Zeolites and catalysis. *Solid State Ionics*. 131 (1-2): 175–188.

Woensdregt C. F. (1983). Structural Morphology of High Sanidine (KAlSi_3O_8). *Zeitschrift Fur Kristallographie*, 162 (1-4): 239–255.

Appendix

1.1 - Dunnett T3, zeolite & iron *in situ* synthesis

Dunnett T3 post hoc test for Si/Al & Fe/Si ratios of products #1-9. *the mean difference is significant at the 0.05 level.

(J) Treatme nt	(I) Treat ment	Mean Difference (I-J)		Std. Error		Sig.		95% Confidence Interval			
		Dependent Variable		Dependent Variable		Dependent Variable		Lower Bound Dependent Variable		Upper Bound Dependent Variable	
		Si/Al	Fe/Si	Si/Al	Fe/Si	Si/Al	Fe/ Si	Si/Al	Fe/ Si	Si/Al	Fe/ Si
1	2	0.059783402	-.104*	0.1283	0.013	1.000	0.01	-0.528	-0.2	0.6473	-0
	3	0.019689595	-.212*	0.1013	0.014	1.000	0	-0.418	-0.3	0.4576	-0.1
	4	-1.34940078 3294392*	0.000	0.0652	0.000	0.000	.	-1.611	0.00	-1.088	0.00
	5	0.173528722	-0.156	0.072	0.068	0.516	0.61	-0.116	-0.5	0.4634	0.20
	6	-0.0171268	-0.157	0.1363	0.084	1.000	0.8	-0.649	-0.6	0.6152	0.28
	7	-5.0335042	0.000	3.2652	0.000	0.925	.	-22.11	0.00	12.045	0.00
	8	-1.49821188 2905940*	-.078*	0.1148	0.012	0.000	0.01	-1.985	-0.1	-1.011	-0
	9	-. 6044934610 00314*	-.116*	0.0856	0.014	0.000	0	-0.934	-0.2	-0.275	-0.1
2	1	-0.0597834	.104*	0.1283	0.013	1.000	0.01	-0.647	0.03	0.5278	0.17
	3	-0.04009381	-.109*	0.146	0.019	1.000	0.01	-0.653	-0.2	0.5733	-0
	4	-1.40918418 5337047*	.104*	0.1237	0.013	0.000	0.01	-2.002	0.03	-0.816	0.17
	5	0.11374532	-0.053	0.1274	0.069	1.000	1	-0.476	-0.4	0.703	0.30
	6	-0.07691021	-0.053	0.1721	0.085	1.000	1	-0.786	-0.5	0.6324	0.38
	7	-5.0932876	.104*	3.2668	0.013	0.920	0.01	-22.16	0.03	11.977	0.17
	8	-1.55799528 4948595*	0.025	0.1557	0.018	0.000	0.98	-2.192	-0.1	-0.924	0.10
	9	-. 6642768630 42969*	-0.013	0.1355	0.020	0.024	1	-1.25	-0.1	-0.079	0.06
3	1	-0.0196896	.212*	0.1013	0.014	1.000	0	-0.458	0.14	0.4182	0.29
	2	0.040093807	.109*	0.146	0.019	1.000	0.01	-0.573	0.03	0.6535	0.19
	4	-1.36909037 8691197*	.212*	0.0954	0.014	0.000	0	-1.805	0.14	-0.934	0.29
	5	0.153839127	0.056	0.1002	0.070	0.946	1	-0.285	-0.3	0.5927	0.41
	6	-0.0368164	0.055	0.1531	0.085	1.000	1	-0.686	-0.4	0.6128	0.49

	7	-5.0531938	.212*	3.2659	0.014	0.923	0	-22.13	0.14	12.022	0.29
	8	-1.51790147 8302746*	.134*	0.1343	0.019	0.000	0	-2.059	0.06	-0.977	0.21
	9	-. 6241830563 97120*	.096*	0.1104	0.020	0.005	0.01	-1.073	0.02	-0.175	0.18
4	1	1.34940078 3294392*	0.000	0.0652	0.000	0.000	.	1.0879	0.00	1.6109	0.00
	2	1.40918418 5337047*	-.104*	0.1237	0.013	0.000	0.01	0.8161	-0.2	2.0022	-0
	3	1.36909037 8691197*	-.212*	0.0954	0.014	0.000	0	0.9336	-0.3	1.8046	-0.1
	5	1.52292950 5728216*	-0.156	0.0634	0.068	0.000	0.61	1.2616	-0.5	1.7842	0.20
	6	1.33227397 8362585*	-0.157	0.132	0.084	0.001	0.8	0.6934	-0.6	1.9712	0.28
	7	-3.68410342	0.000	3.265	0.000	0.993	.	-20.76	0.00	13.395	0.00
	8	-0.1488111	-.078*	0.1097	0.012	0.980	0.01	-0.634	-0.1	0.336	-0
	9	. 7449073222 94178*	-.116*	0.0785	0.014	0.000	0	0.4367	-0.2	1.0531	-0.1
	5	1	-0.17352872	0.156	0.072	0.068	0.516	0.61	-0.463	-0.2	0.1163
2		-0.11374532	0.053	0.1274	0.069	1.000	1	-0.703	-0.3	0.4755	0.40
3		-0.15383913	-0.056	0.1002	0.070	0.946	1	-0.593	-0.4	0.285	0.29
4		-1.52292950 5728216*	0.156	0.0634	0.068	0.000	0.61	-1.784	-0.2	-1.262	0.51
6		-0.19065553	-0.001	0.1354	0.108	0.967	1	-0.825	-0.5	0.4434	0.45
7		-5.20703292	0.156	3.2651	0.068	0.909	0.61	-22.29	-0.2	11.871	0.51
8		-1.67174060 5339765*	0.078	0.1139	0.069	0.000	0.99	-2.159	-0.3	-1.184	0.43
9		-. 7780221834 34138*	0.040	0.0843	0.070	0.000	1	-1.106	-0.3	-0.45	0.39
6		1	0.017126805	0.157	0.1363	0.084	1.000	0.8	-0.615	-0.3	0.6494
	2	0.076910207	0.053	0.1721	0.085	1.000	1	-0.632	-0.4	0.7862	0.49
	3	0.0368164	-0.055	0.1531	0.085	1.000	1	-0.613	-0.5	0.6864	0.38
	4	-1.33227397 8362585*	0.157	0.132	0.084	0.001	0.8	-1.971	-0.3	-0.693	0.59
	5	0.190655527	0.001	0.1354	0.108	0.967	1	-0.443	-0.5	0.8247	0.45
	7	-5.01637739	0.157	3.2672	0.084	0.927	0.8	-22.09	-0.3	12.053	0.59
	8	-1.48108507 7974133*	0.079	0.1623	0.084	0.000	1	-2.147	-0.4	-0.815	0.51
	9	-0.58736666	0.041	0.1431	0.085	0.071	1	-1.215	-0.4	0.0407	0.47

7	1	5.0335042	0.000	3.2652	0.000	0.925	.	-12.04	0.00	22.112	0.00
	2	5.093287602	-.104*	3.2668	0.013	0.920	0.01	-11.98	-0.2	22.164	-0
	3	5.053193795	-.212*	3.2659	0.014	0.923	0	-12.02	-0.3	22.128	-0.1
	4	3.684103416	0.000	3.265	0.000	0.993	.	-13.4	0.00	20.763	0.00
	5	5.207032922	-0.156	3.2651	0.068	0.909	0.61	-11.87	-0.5	22.286	0.20
	6	5.016377395	-0.157	3.2672	0.084	0.927	0.8	-12.05	-0.6	22.085	0.28
	8	3.535292317	-.078*	3.2663	0.012	0.996	0.01	-13.54	-0.1	20.608	-0
	9	4.429010739	-.116*	3.2654	0.014	0.968	0	-12.65	-0.2	21.506	-0.1
	8	1	1.49821188 2905940*	.078*	0.1148	0.012	0.000	0.01	1.0111	0.02	1.9853
2		1.55799528 4948595*	-0.025	0.1557	0.018	0.000	0.98	0.9241	-0.1	2.1919	0.05
3		1.51790147 8302746*	-.134*	0.1343	0.019	0.000	0	0.9766	-0.2	2.0592	-0.1
4		0.1488111	.078*	0.1097	0.012	0.980	0.01	-0.336	0.02	0.6336	0.14
5		1.67174060 5339765*	-0.078	0.1139	0.069	0.000	0.99	1.1841	-0.4	2.1594	0.27
6		1.48108507 7974133*	-0.079	0.1623	0.084	0.000	1	0.8147	-0.5	2.1475	0.35
7		-3.53529232	.078*	3.2663	0.012	0.996	0.01	-20.61	0.02	13.538	0.14
9		. 8937184219 05726*	-0.038	0.1229	0.019	0.001	0.76	0.3977	-0.1	1.3898	0.03
9		1	. 6044934610 00314*	.116*	0.0856	0.014	0.000	0	0.2754	0.05	0.9336
	2	. 6642768630 42969*	0.013	0.1355	0.020	0.024	1	0.0786	-0.1	1.2499	0.09
	3	. 6241830563 97120*	-.096*	0.1104	0.020	0.005	0.01	0.1754	-0.2	1.073	-0
	4	-. 7449073222 94178*	.116*	0.0785	0.014	0.000	0	-1.053	0.05	-0.437	0.18
	5	. 7780221834 34138*	-0.040	0.0843	0.070	0.000	1	0.4501	-0.4	1.106	0.31
	6	0.587366656	-0.041	0.1431	0.085	0.071	1	-0.041	-0.5	1.2154	0.39
	7	-4.42901074	.116*	3.2654	0.014	0.968	0	-21.51	0.05	12.648	0.18
	8	-. 8937184219 05726*	0.038	0.1229	0.019	0.001	0.76	-1.39	-0	-0.398	0.11

1.2 - Dunnett T3, Phillipsite treatments

Dunnett T3 post hoc test for Si/Al & Fe/Si ratios of Phillipsite treatments. The treatments are 1) Phillipsite, 2) HNO₃ +Fe³⁺, 3)NH₄HCO₃ + Fe³⁺, 4) Fe³⁺, 5) HNO₃, 6) NH₄HCO₃.

*the mean difference is significant at the 0.05 level.

(J) Treatment	(I) Treatment	Mean Difference (I-J)		Std. Error		Sig.		95% Confidence Interval			
		Dependent Variable		Dependent Variable		Dependent Variable		Lower Bound Dependent Variable		Upper Bound Dependent Variable	
		Si/Al	Fe/Si	Si/Al	Fe/Si	Si/Al	Fe/Si	Si/Al	Fe/Si	Si/Al	Fe/Si
1	2	-40.576	-0.008	20.2054	0.004	0.566	0.43	-127	-0	45.804	0.01
	3	0.211392	-.027*	0.061943	0.006	0.073	0.04	-0.015	-0.1	0.4377	0.00
	4	0.1633	-0.033	0.093291	0.015	0.704	0.44	-0.176	-0.1	0.5027	0.03
	5	-58.0646	0.000	25.6876	0.000	0.444	.	-167.9	0.00	51.753	0.00
	6	0.06871	0.000	0.093151	0.000	0.999	.	-0.27	0.00	0.4075	0.00
2	1	40.576	0.008	20.2054	0.004	0.566	0.43	-45.8	-0	126.96	0.02
	3	40.7874	-0.019	20.20536	0.007	0.561	0.22	-45.59	-0	127.17	0.01
	4	40.7393	-0.025	20.20548	0.015	0.562	0.76	-45.64	-0.1	127.12	0.04
	5	-17.4886	0.008	32.68188	0.004	1.000	0.43	-134.4	-0	99.439	0.02
	6	40.6447	0.008	20.20548	0.004	0.564	0.43	-45.74	-0	127.02	0.02
3	1	-0.21139	.027*	0.061943	0.006	0.073	0.04	-0.438	0.00	0.015	0.05
	2	-40.7874	0.019	20.20536	0.007	0.561	0.22	-127.2	-0	45.593	0.04
	4	-0.04809	-0.006	0.084461	0.016	1.000	1	-0.375	-0.1	0.2784	0.06
	5	-58.276	.027*	25.68757	0.006	0.440	0.04	-168.1	0.00	51.542	0.05
	6	-0.14268	.027*	0.084306	0.006	0.737	0.04	-0.468	0.00	0.1831	0.05
4	1	-0.1633	0.033	0.093291	0.015	0.704	0.44	-0.503	-0	0.1761	0.10
	2	-40.7393	0.025	20.20548	0.015	0.562	0.76	-127.1	-0	45.641	0.09
	3	0.04809	0.006	0.084461	0.016	1.000	1	-0.278	-0.1	0.3746	0.07
	5	-58.2279	0.033	25.68766	0.015	0.441	0.44	-168	-0	51.59	0.10
	6	-0.0946	0.033	0.109425	0.015	0.997	0.44	-0.482	-0	0.2928	0.10
5	1	58.0646	0.000	25.6876	0.000	0.444	.	-51.75	0.00	167.88	0.00
	2	17.4886	-0.008	32.68188	0.004	1.000	0.43	-99.44	-0	134.42	0.01
	3	58.276	-.027*	25.68757	0.006	0.440	0.04	-51.54	-0.1	168.09	0.00
	4	58.2279	-0.033	25.68766	0.015	0.441	0.44	-51.59	-0.1	168.05	0.03
	6	58.1333	0.000	25.68766	0.000	0.443	.	-51.68	0.00	167.95	0.00
6	1	-0.06871	0.000	0.093151	0.000	0.999	.	-0.407	0.00	0.2701	0.00
	2	-40.6447	-0.008	20.20548	0.004	0.564	0.43	-127	-0	45.736	0.01
	3	0.14268	-.027*	0.084306	0.006	0.737	0.04	-0.183	-0.1	0.4685	0.00
	4	0.0946	-0.033	0.109425	0.015	0.997	0.44	-0.293	-0.1	0.482	0.03
	5	-58.1333	0.000	25.68766	0.000	0.443	.	-168	0.00	51.684	0.00

1.3 - Dunnett T3, Analcime treatments

Dunnett T3 post hoc test for Si/Al & Fe/Si ratios of Analcime treatments. The treatments are 1) Analcime, 2) HNO₃ +Fe³⁺, 3)NH₄HCO₃ + Fe³⁺, 4) Fe³⁺, 5) HNO₃, 6) NH₄HCO₃.

*the mean difference is significant at the 0.05 level.

(J) Treatme nt	(I) Treat ment	Mean Difference (I-J)		Std. Error		Sig.		95% Confidence Interval			
		Dependent Variable		Dependent Variable		Dependent Variable		Lower Bound Dependent Variable		Upper Bound Dependent Variable	
		Si/Al	Fe/Si	Si/Al	Fe/Si	Si/Al	Fe/Si	Si/Al	Fe/Si	Si/Al	Fe/Si
1	2	-1.74587366 4190593*	.197*	0.040741	0.007	0	0	-1.912	0.17	-1.58	0.23
	3	-1.73492161 5006308*	.176*	0.041099	0.027	0	0.01	-1.901	0.06	-1.569	0.29
	4	-0.34467386	.128*	0.653945	0.024	1	0.02	-3.133	0.02	2.4434	0.23
	5	-1.71101541 4738633*	.216*	0.040899	0.006	0	0	-1.877	0.19	-1.545	0.24
	6	-1.72406745 8700522*	.186*	0.039592	0.027	0	0	-1.892	0.07	-1.557	0.3
2	1	1.745873664 190593*	-.197*	0.040741	0.007	0	0	1.58	-0.2	1.9118	-0.2
	3	0.010952049	-0.021	0.016111	0.028	1	1	-0.046	-0.1	0.0681	0.09
	4	1.401199805	-0.069	0.652851	0.025	0.497	0.25	-1.389	-0.2	4.1917	0.03
	5	0.034858249	0.019	0.015594	0.009	0.407	0.49	-0.02	-0	0.0901	0.05
	6	0.021806205	-0.011	0.011748	0.027	0.642	1	-0.023	-0.1	0.0671	0.1
3	1	1.734921615 006308*	-.176*	0.041099	0.027	0	0.01	1.5693	-0.3	1.9006	-0.1
	2	-0.01095205	0.021	0.016111	0.028	1	1	-0.068	-0.1	0.0462	0.13
	4	1.390247756	-0.048	0.652873	0.036	0.505	0.93	-1.4	-0.2	4.1807	0.08
	5	0.0239062	0.04	0.016505	0.028	0.874	0.85	-0.035	-0.1	0.0824	0.15
	6	0.010854156	0.01	0.012933	0.038	0.997	1	-0.04	-0.1	0.0614	0.14
4	1	0.344673859	-.128*	0.653945	0.024	1	0.02	-2.443	-0.2	3.1328	-0
	2	-1.401199805	0.069	0.652851	0.025	0.497	0.25	-4.192	-0	1.3893	0.17
	3	-1.39024776	0.048	0.652873	0.036	0.505	0.93	-4.181	-0.1	1.4002	0.18
	5	-1.36634156	0.088	0.652861	0.025	0.523	0.1	-4.157	-0	1.4241	0.19
	6	-1.3793936	0.058	0.65278	0.036	0.513	0.8	-4.17	-0.1	1.4112	0.19

5	1	1.711015414 738633*	-.216*	0.040899	0.006	0	0	1.5452	-0.2	1.8768	-0.2
	2	-0.03485825	-0.019	0.015594	0.009	0.407	0.49	-0.09	-0.1	0.0204	0.01
	3	-0.0239062	-0.04	0.016505	0.028	0.874	0.85	-0.082	-0.2	0.0346	0.07
	4	1.366341556	-0.088	0.652861	0.025	0.523	0.1	-1.424	-0.2	4.1568	0.01
	6	-0.01305204	-0.03	0.012283	0.027	0.979	0.97	-0.061	-0.1	0.0346	0.08
6	1	1.724067458 700522*	-.186*	0.039592	0.027	0	0	1.5566	-0.3	1.8915	-0.1
	2	-0.02180621	0.011	0.011748	0.027	0.642	1	-0.067	-0.1	0.0234	0.12
	3	-0.01085416	-0.01	0.012933	0.038	0.997	1	-0.061	-0.1	0.0397	0.12
	4	1.3793936	-0.058	0.65278	0.036	0.513	0.8	-1.411	-0.2	4.17	0.07
	5	0.013052044	0.03	0.012283	0.027	0.979	0.97	-0.035	-0.1	0.0607	0.14

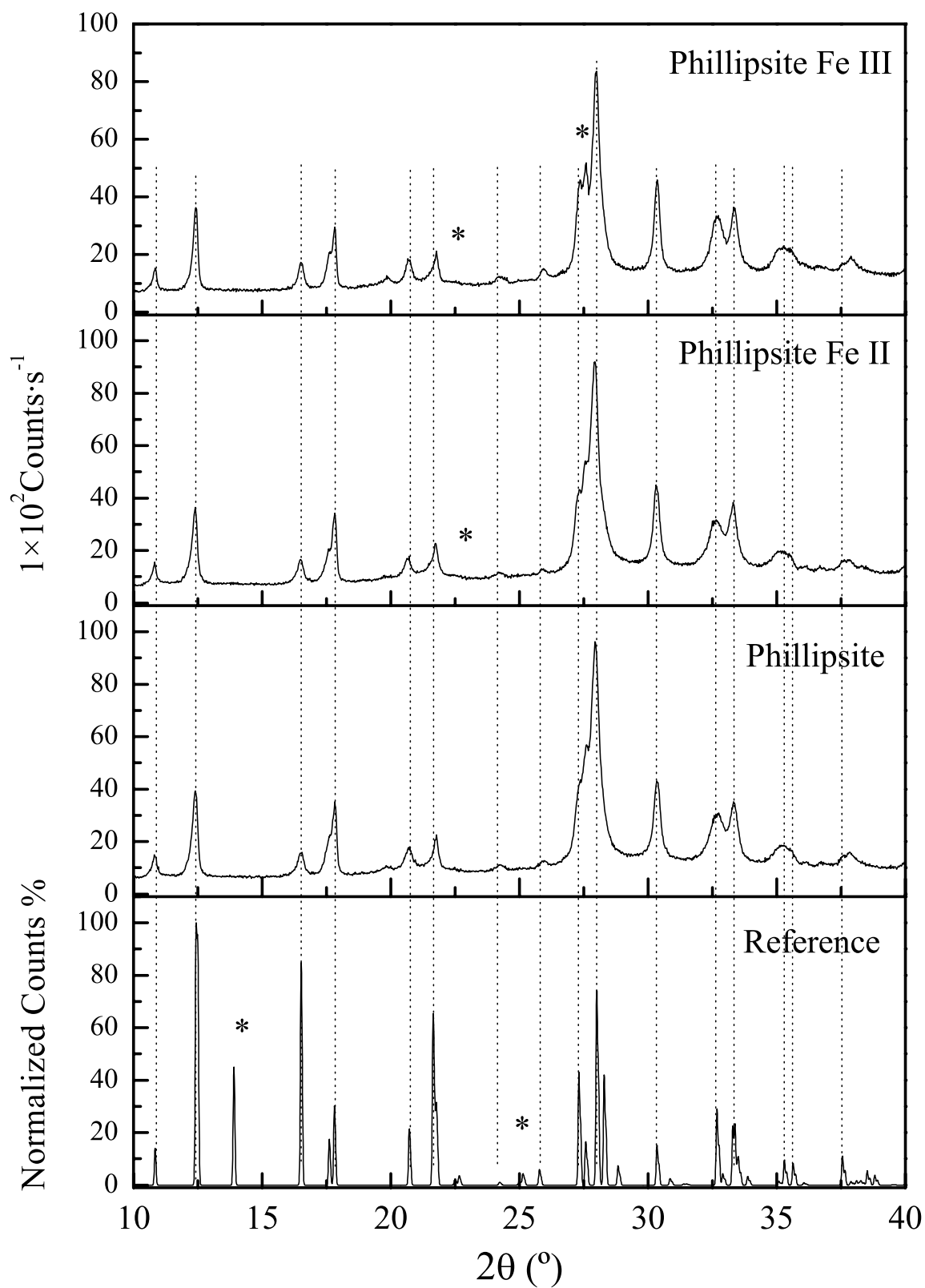
1.4 - Dunnett T3, Sanidine treatments

Dunnett T3 post hoc test for Si/Al & Fe/Si ratios of Sanidine treatments. The treatments are 1) Sanidine, 2) HNO₃ +Fe³⁺, 3)NH₄HCO₃ + Fe³⁺, 4) Fe³⁺, 5) HNO₃, 6) NH₄HCO₃.

*the mean difference is significant at the 0.05 level.

(J) Treatme nt	(I) Treat ment	Mean Difference (I- J)		Std. Error		Sig.		95% Confidence Interval			
		Dependent Variable		Dependent Variable		Dependent Variable		Lower Bound Dependent Variable		Upper Bound Dependent Variable	
		Si/Al	Fe/Si	Si/Al	Fe/Si	Si/Al	Fe/ Si	Si/Al	Fe/ Si	Si/Al	Fe/ Si
1	2	3.57102	-0.015	3.268316	0.005	0.964	0.16	-11.47	-0	18.61	0.00
	3	3.548115	-0.020	3.270979	0.006	0.966	0.18	-11.48	-0.1	18.577	0.01
	4	3.63929	-0.014	3.265301	0.009	0.959	0.77	-11.41	-0.1	18.689	0.02
	5	3.46497	0.000	3.265983	0.000	0.970	.	-11.58	0.00	18.512	0.00
	6	3.55139	0.000	3.267351	0.000	0.965	.	-11.49	0.00	18.594	0.00
2	1	-3.57102	0.015	3.268316	0.005	0.964	0.16	-18.61	0.00	11.468	0.03
	3	-0.02291	-0.005	0.253277	0.008	1.000	1	-0.932	-0	0.8864	0.02
	4	0.06827	0.001	0.164418	0.010	1.000	1	-0.575	-0	0.7117	0.04
	5	-0.10605	0.015	0.177447	0.005	1.000	0.16	-0.763	0.00	0.5506	0.03
	6	-0.01963	0.015	0.201069	0.005	1.000	0.16	-0.735	0.00	0.6955	0.03
3	1	-3.54812	0.020	3.270979	0.006	0.966	0.18	-18.58	-0	11.481	0.05
	2	0.02291	0.005	0.253277	0.008	1.000	1	-0.886	-0	0.9322	0.03
	4	0.09118	0.006	0.210829	0.011	1.000	1	-0.76	-0	0.9425	0.05
	5	-0.08315	0.020	0.22114	0.006	1.000	0.18	-0.935	-0	0.7685	0.05
	6	0.00327	0.020	0.240509	0.006	1.000	0.18	-0.876	-0	0.8823	0.05
4	1	-3.63929	0.014	3.265301	0.009	0.959	0.77	-18.69	-0	11.411	0.05
	2	-0.06827	-0.001	0.164418	0.010	1.000	1	-0.712	-0	0.5752	0.04
	3	-0.09118	-0.006	0.210829	0.011	1.000	1	-0.943	-0.1	0.7602	0.03
	5	-0.17433	0.014	0.108567	0.009	0.790	0.77	-0.569	-0	0.2206	0.05
	6	-0.08791	0.014	0.143973	0.009	1.000	0.77	-0.639	-0	0.4636	0.05
5	1	-3.46497	0.000	3.265983	0.000	0.970	.	-18.51	0.00	11.582	0.00
	2	0.10605	-0.015	0.177447	0.005	1.000	0.16	-0.551	-0	0.7627	0.00
	3	0.08315	-0.020	0.22114	0.006	1.000	0.18	-0.769	-0.1	0.9348	0.01
	4	0.17433	-0.014	0.108567	0.009	0.790	0.77	-0.221	-0.1	0.5692	0.02
	6	0.08642	0.000	0.15869	0.000	1.000	.	-0.489	0.00	0.6618	0.00
6	1	-3.55139	0.000	3.267351	0.000	0.965	.	-18.59	0.00	11.491	0.00
	2	0.01963	-0.015	0.201069	0.005	1.000	0.16	-0.696	-0	0.7348	0.00
	3	-0.00327	-0.020	0.240509	0.006	1.000	0.18	-0.882	-0.1	0.8757	0.01
	4	0.08791	-0.014	0.143973	0.009	1.000	0.77	-0.464	-0.1	0.6394	0.02
	5	-0.08642	0.000	0.15869	0.000	1.000	.	-0.662	0.00	0.489	0.00

2.1 - PXRD, Phillipsite & iron *in situ*



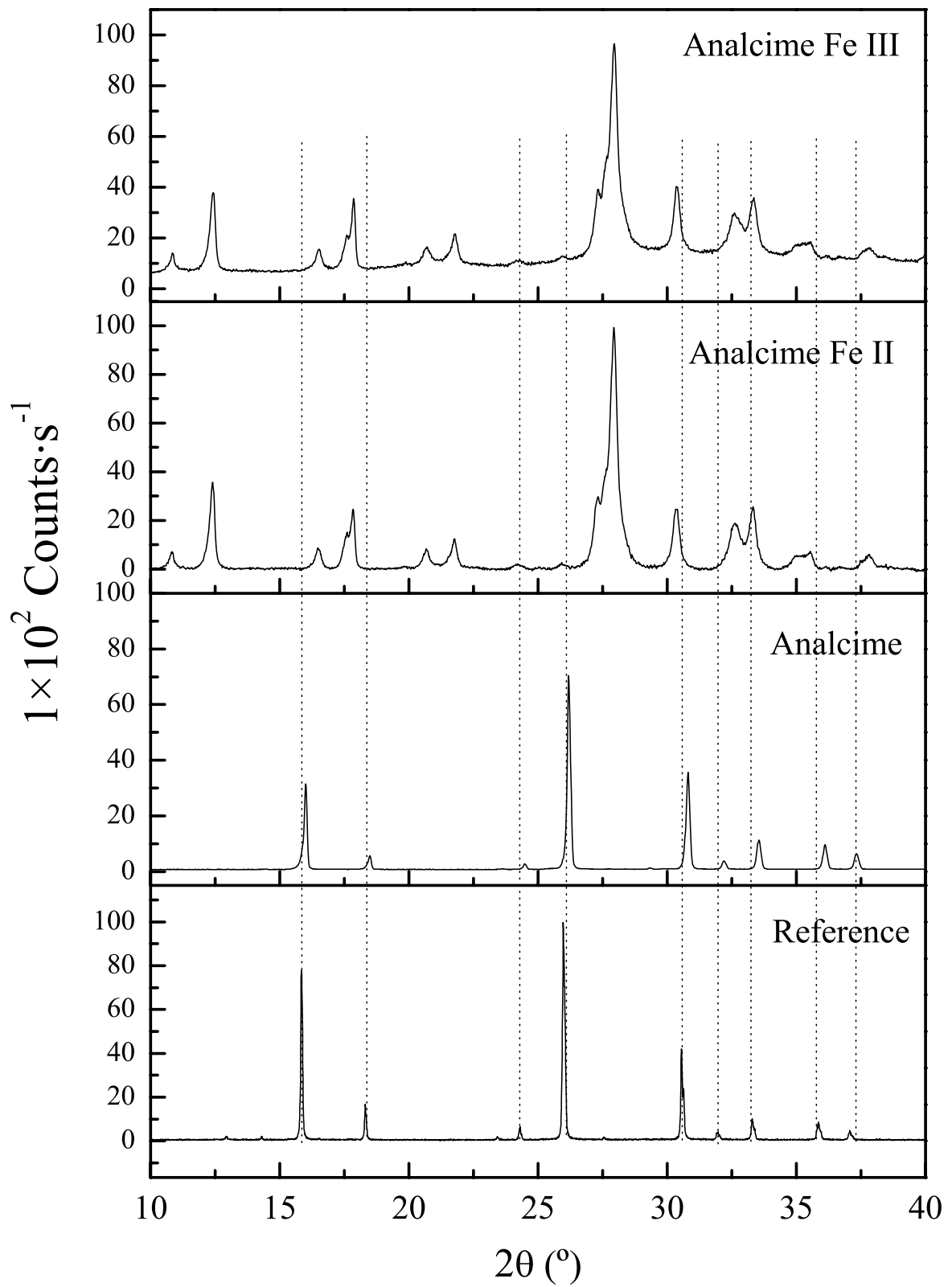
PXRD spectra of phillipsite and iron *in situ* with reference (Chen *et al.* 2002)

2.2 - PXRD, crystallographic information, phillipsite

Crystallographic information from PXRD data with phillipsite reference (Chen *et al.* 2002)

hkl	Phillipsite reference		Phillipsite		Phillipsite Fe II		Phillipsite Fe III	
	d(Å)	I/I ₀	d(Å)	I/I ₀	d(Å)	I/I ₀	d(Å)	I/I ₀
101	8.24	22.00	8.16	9.10	8.17	10.99	8.15	11.51
002	7.15	56.00	7.12	36.42	7.13	35.82	7.12	40.91
121	5.40	30.00	5.36	10.31	5.37	11.34	5.36	12.43
022	5.03	33.00	5.05	15.41	5.05	15.99	5.04	17.35
200	-	-	4.97	29.86	4.97	31.52	4.98	29.83
103	4.31	12.00	4.48	3.69	-	-	4.46	4.42
113	-	-	4.29	11.74	24.30	10.75	4.30	12.05
220	4.10	26.00	4.08	16.25	4.09	17.85	4.08	16.87
123	3.67	5.00	3.67	3.64	3.67	3.34	3.68	3.48
014	-	-	3.43	4.96	3.44	4.48	3.44	6.72
141	3.25	44.00	3.27	35.04	3.27	37.21	3.27	45.58
301	-	-	3.23	55.00	3.24	54.51	3.23	58.06
024	3.25	44.00	3.19	100.00	3.19	100.00	3.18	100.00
321	-	-	2.95		2.95	40.66	2.94	47.40

2.3 - PXRD, Analcime & iron *in situ*



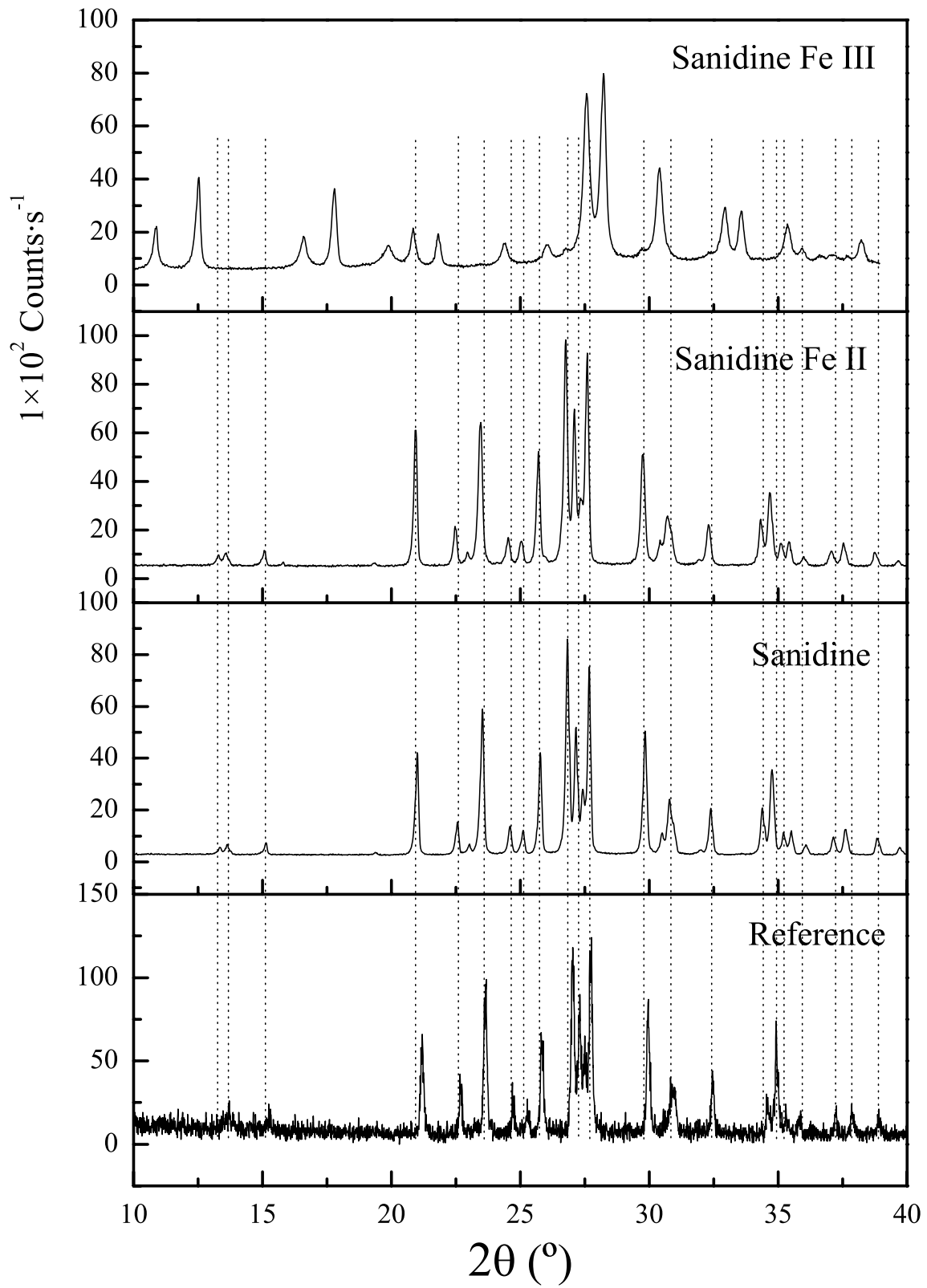
PXRD spectra of analcime and iron *in situ* with reference (Joshi *et al.* 1983)

2.4 - PXRD, crystallographic information, analcime

Crystallographic information from PXRD data with analcime reference (Joshi *et al.* 1983)

hkl	Analcime reference		Analcime		Analcime Fe II		Analcime Fe III		Phillipsite reference		
	d(Å)	I/I ₀	d(Å)	I/I ₀	d(Å)	I/I ₀	d(Å)	I/I ₀	hkl	d(Å)	I/I ₀
211	5.57	57.00	5.36	44.15	8.15	7.12	8.15	8.57	101	8.24	22.00
220	4.82	17.00	4.80	7.00	7.12	33.58	7.11	38.06	002	7.15	56.00
321	3.65	13.00	3.64	2.85	5.37	8.74	5.36	9.76	121	5.40	30.00
400	3.41	100.00	3.40	100.00	5.04	15.30	5.04	16.05	022	5.03	33.00
411	3.20	15.00	3.04	0.24	-	-			200	-	-
332	2.92	53.00	2.90	50.25	4.29	8.37	4.28	8.59	103	4.31	12.00
422	2.78	11.00	2.78	4.31					113	-	-
431	2.67	20.00	2.67	15.19	4.07	12.42	4.08	14.10	220	4.10	26.00
521	2.49	16.00	2.49	12.65					032	-	-
440	2.41	12.00	2.41	7.91	3.69	1.23	3.68	2.57	123	3.67	5.00
661	2.22	11.00			3.52	0.31	3.53	0.84	004	3.53	4.00
620	2.16	6.00			3.23	37.50	3.26	31.86	141	3.25	44.00
541	2.10	8.00					3.23	37.94	024	3.25	44.00
640	1.90	13.00			3.19	100.00	3.18	100.00	311	3.18	100.00
633	1.86	11.00			2.94	24.59	2.94	31.21	240	2.95	33.00

2.5 - PXRD, Sanidine & iron *in situ*



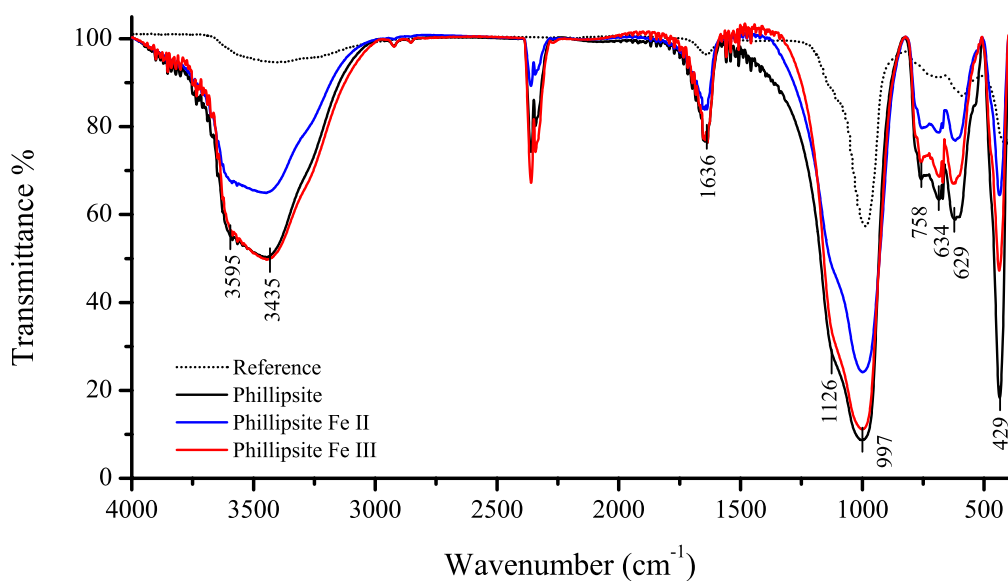
PXRD spectra of Sanidine and iron *in situ* sanidine with reference (Woensdrecht 1983)

2.6 - PXRD, crystallographic information, sanidine

Crystallographic information from PXRD data with sanidine (Woensdrecht 1983, & Goldsmith & Laves 1954) and merlinoite reference (Passaglia *et al.* 1977)

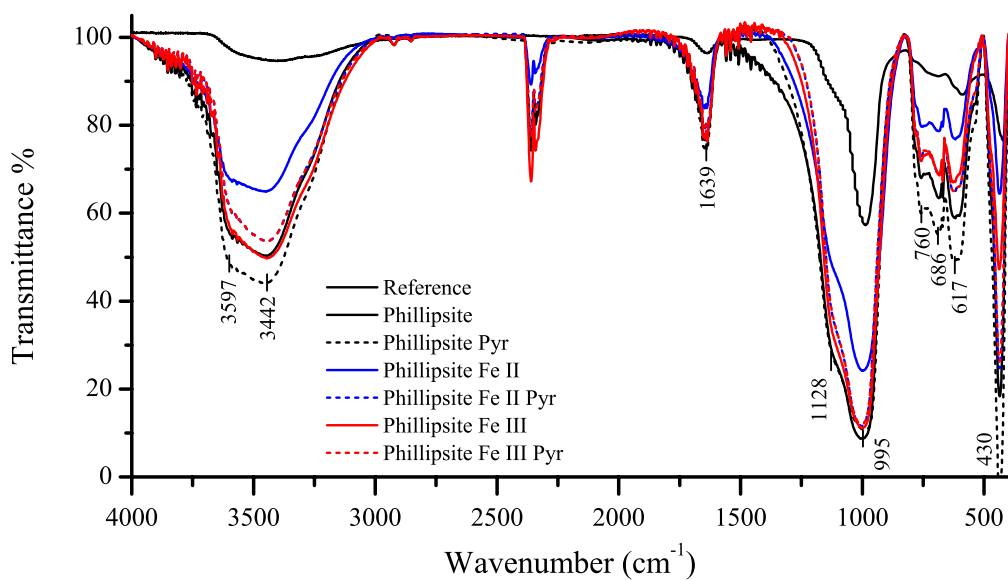
hkl	Sanidine reference		Sanidine		Sanidine Fe II		Sanidine Fe III		Merlinoite reference		
	d(Å)	I/I ₀	d(Å)	I/I ₀	d(Å)	I/I ₀	d(Å)	I/I ₀	hkl	d(Å)	I/I ₀
110	6.63	10.00	6.63	3.18	6.66	4.64	10.04	1.66	110	10.02	12.76
001	6.45	10.00	-	-	-	-	8.13	22.17	011	8.15	23.13
020	6.52	10.00	6.49	4.58	6.52	5.16	7.05	45.46	020	7.11	61.77
130	3.78	100.00	3.78	67.29	3.79	63.35	-	-	200	7.06	58.69
021	4.58	20.00	4.58	1.16	4.59	1.16	5.34	16.49	121	5.35	77.19
201	4.22	80.00	4.23	47.78	4.24	59.98	4.99	40.99	002	4.97	43.21
111	5.59	30.00	5.85	5.74	5.61	1.64	4.46	11.31	310	4.47	28.19
221	3.54	30.00	3.55	10.43	3.56	10.89	4.26	19.07	301	4.25	1.30
112	3.46	80.00	3.46	46.54	3.47	50.22	4.07	17.48	022	4.08	12.54
200	3.85	10.00	3.86	4.44	3.88	6.12	3.64	11.41	321	3.65	31.88
202	3.28	90.00	3.32	100.00	3.33	100.00	3.23	89.49	141	3.26	56.67
							3.16	100.00	240	3.18	100.00
							2.94	50.81	123	2.94	55.60
							2.72	30.02	033	2.72	27.36
							2.67	27.80	422	2.67	13.32
							2.54	20.37	521	2.54	11.93

3.1.1 - FTIR: Phillipsite & iron *in situ*



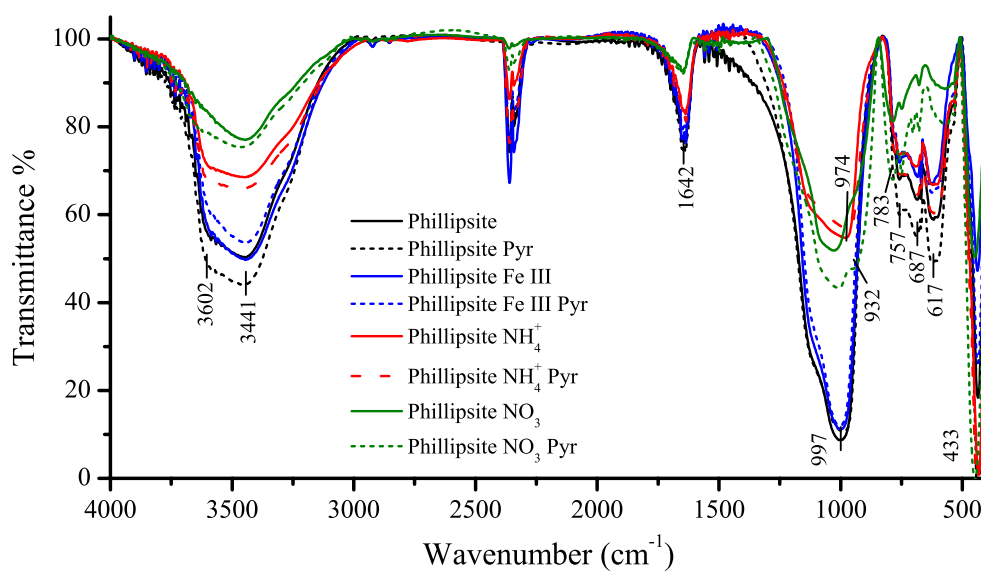
Phillipsite & iron *in situ* synthesised product with reference.

3.1.2 - FTIR: Phillipsite & iron *in situ* - pyridine



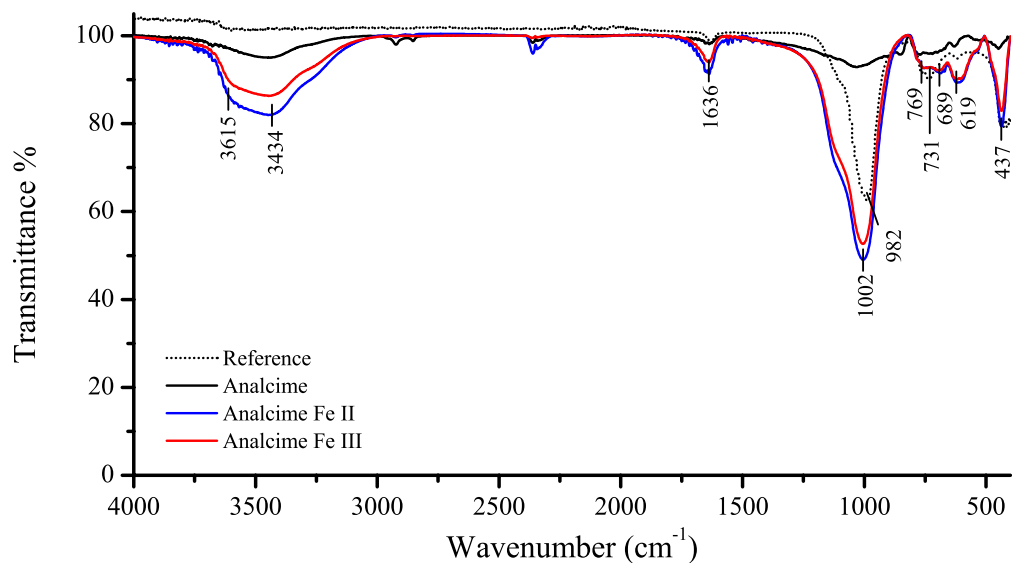
Phillipsite & iron *in situ* pyridine series with reference.

3.1.3 - FTIR: Phillipsite post synthesis treated - pyridine



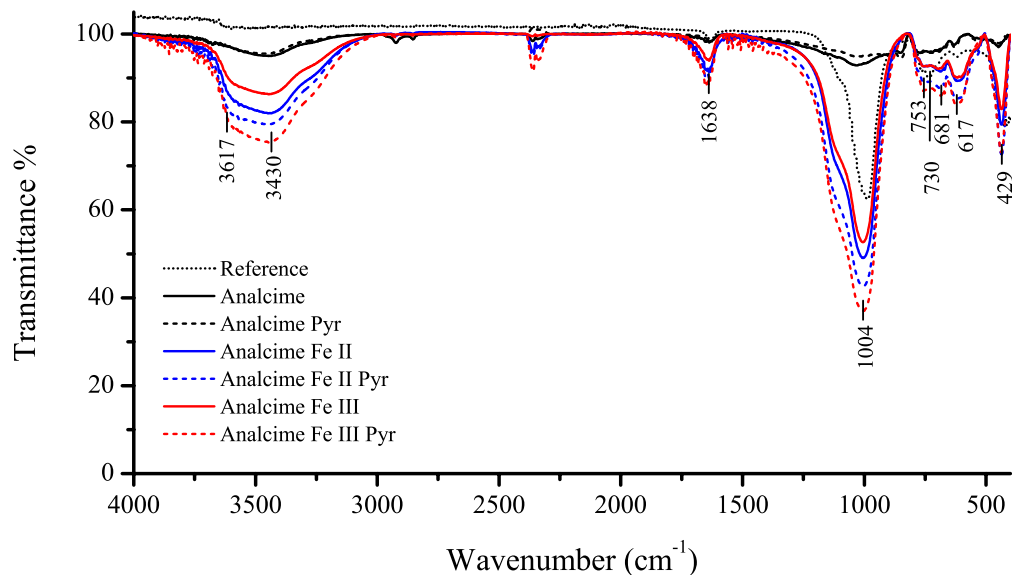
Phillipsite iron modification pyridine series with synthesised phillipsite as a reference.

3.2.1 - FTIR: Analcime & iron *in situ* - pyridine



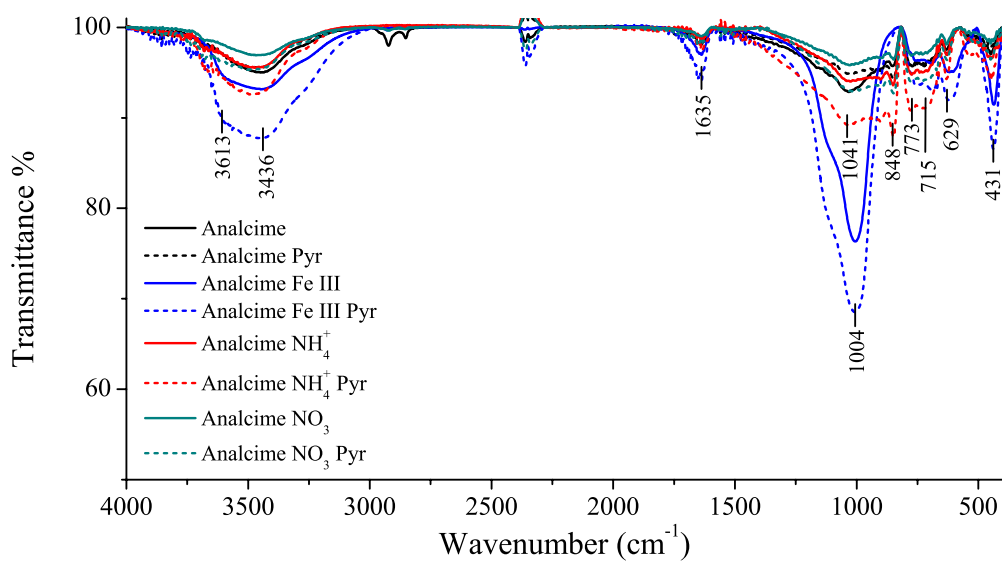
Analcime & iron *in situ* synthesised product with reference.

3.2.2 - FTIR: Analcime & iron *in situ* - pyridine



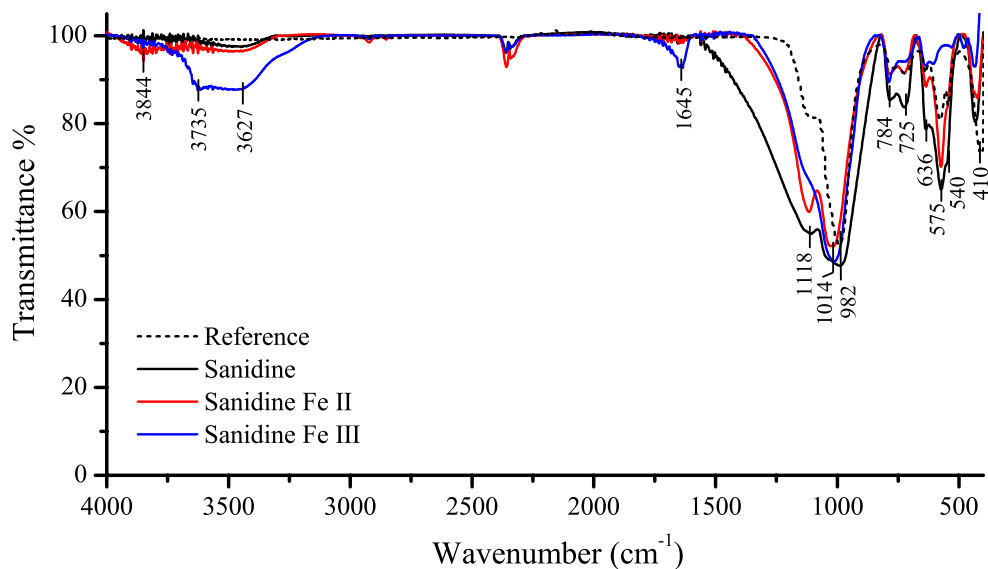
Analcime & iron *in situ* pyridine series with reference.

3.2.3 - FTIR: Analcime post synthesis treated - pyridine



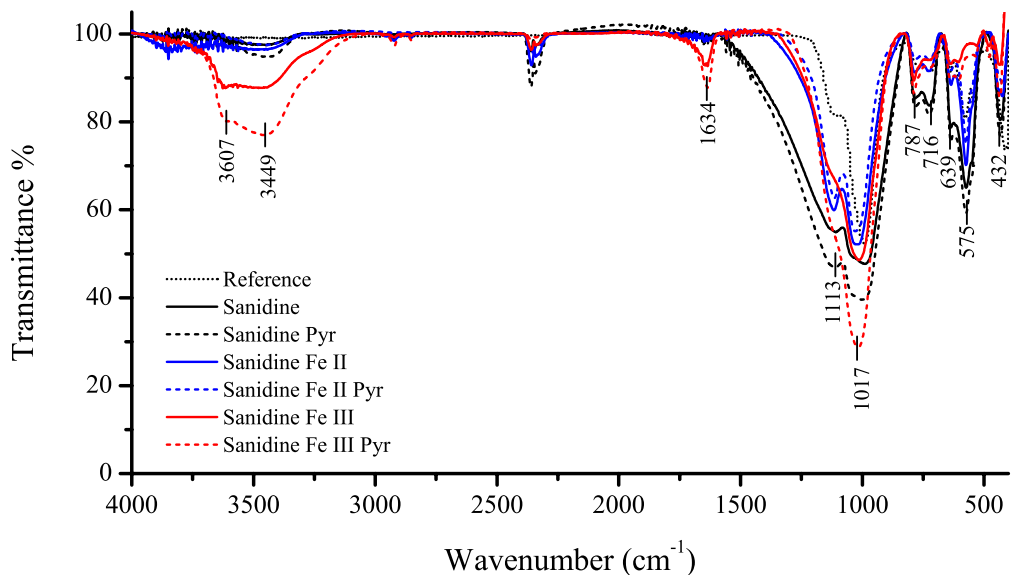
Analcime iron modification pyridine series with synthesised analcime as a reference.

3.3.1 - FTIR: Sanidine & iron *in situ*



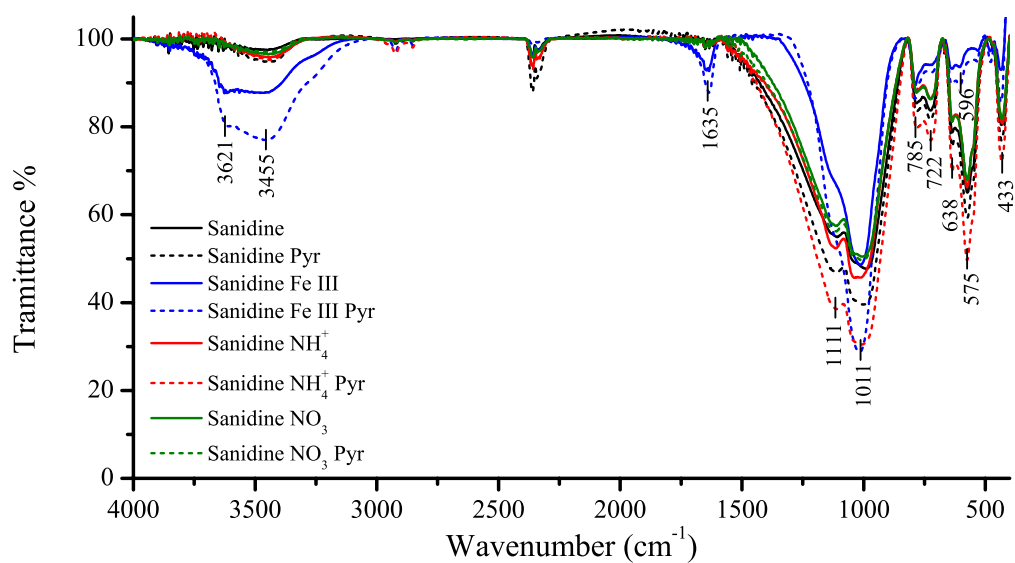
Sanidine & iron *in situ* synthesised product with reference.

3.3.2 - FTIR: Sanidine & iron *in situ* - pyridine



Sanidine & iron *in situ* pyridine series with reference.

3.3.3 - FTIR: Sanidine post synthesis treated - pyridine



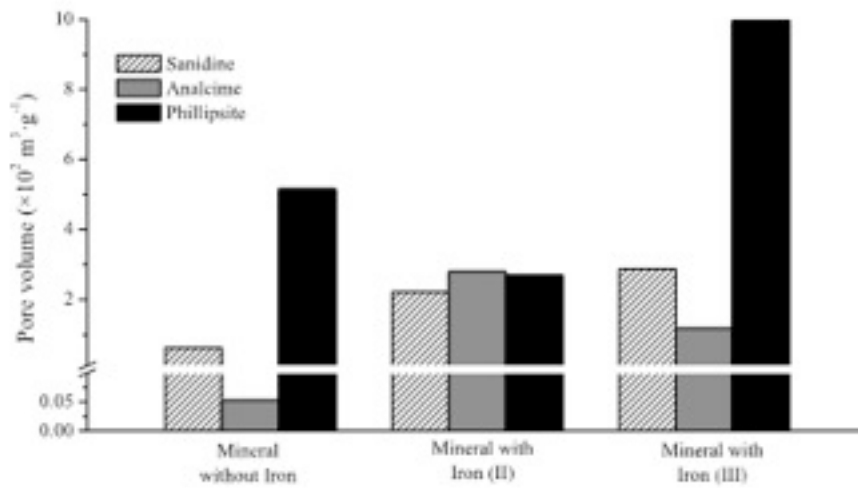
Sanidine iron modification pyridine series with synthesised sanidine as a reference.

3.4 - Infra red band assignation table.

Assignation table of all peaks seen in FTIR with references.

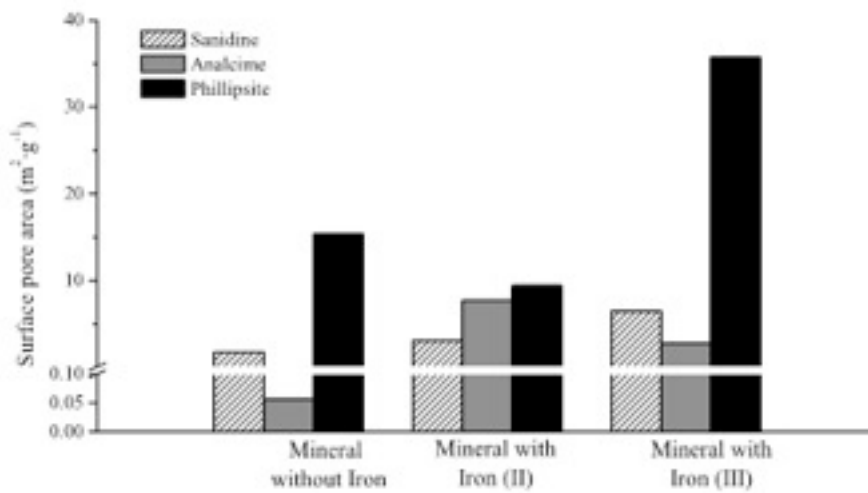
Wavenumber (cm ⁻¹)	Assignment	Reference
3800	Isolated (SiOH)	Ates & Hardacre 2012
3780	AIOH	Dzwigaj <i>et al.</i> 2000
3700	Zeolitic water	Ates & Hardacre 2012
3660	Isolated OH ⁻ , Stretching and AIOH	Ates & Hardacre 2012, Dzwigaj <i>et al.</i> 2000
3640	OH stretching region * With pyridine the broadening of OH at 3640 disappears but 3550	Weitkamp 2000
3609	AIOH	Dzwigaj <i>et al.</i> 2000
3550	OH stretching region	Weitkamp 2000, Joshi <i>et al.</i> 1983
3400	Isolated (Si-O(H)-Al)	Ates & Hardacre 2012
1650	Water band H ₂ O	Joshi <i>et al.</i> 1983, Ates & Hardacre 2012
1540	Is due to the formation of bonds with pyridine ions adsorbed on Brønsted acid groups	Weitkamp 2000
1510	Water band H ₂ O	Joshi <i>et al.</i> 1983
1455	Lewis acid sites	Weitkamp 2000
1229	Existence of pores with 3D channels	Kim & Chung 2003
1124	Asymmetric stretch (Si-O(Si))	Joshi <i>et al.</i> 1983, Anbalagan <i>et al.</i> 2009
1060	Asymmetric stretch (Si-O(Si))	Joshi <i>et al.</i> 1983, Anbalagan <i>et al.</i> 2009
1028	Vibration (Si-O(Al))	Anbalagan <i>et al.</i> 2009
1010	Vibration (Si-O(Al))	Anbalagan <i>et al.</i> 2009
780	Symmetric stretch (Si ₂ O)	Joshi <i>et al.</i> 1983, Anbalagan <i>et al.</i> 2009
745	Symmetric stretch (Al-O(Al))	Joshi <i>et al.</i> 1983, Anbalagan <i>et al.</i> 2009
710	Symmetric stretch (Al-O(Al))	Joshi <i>et al.</i> 1983, Anbalagan <i>et al.</i> 2009
630	Double ring, Tetrahedral ring vibrations	Joshi <i>et al.</i> 1983, Anbalagan <i>et al.</i> 2009
583	Tetrahedral ring vibrations	Anbalagan <i>et al.</i> 2009
546	Indicative of formation of double 5 rings (D5R) by tetrahedral SiO ₄ and AlO ₄	Kim & Chung 2003
495	Al or Si-O bond (O-Si(Al)-O)	Joshi <i>et al.</i> 1983, Anbalagan <i>et al.</i> 2009
450	Al or Si-O bond (O-Si(Al)-O)	Joshi <i>et al.</i> 1983, Anbalagan <i>et al.</i> 2009
447	Internal vibrations of Si and AlO ₄ tetrahedral	Kim & Chung 2003
400	Pore opening	Joshi <i>et al.</i> 1983

4.1 - BET Pore volume



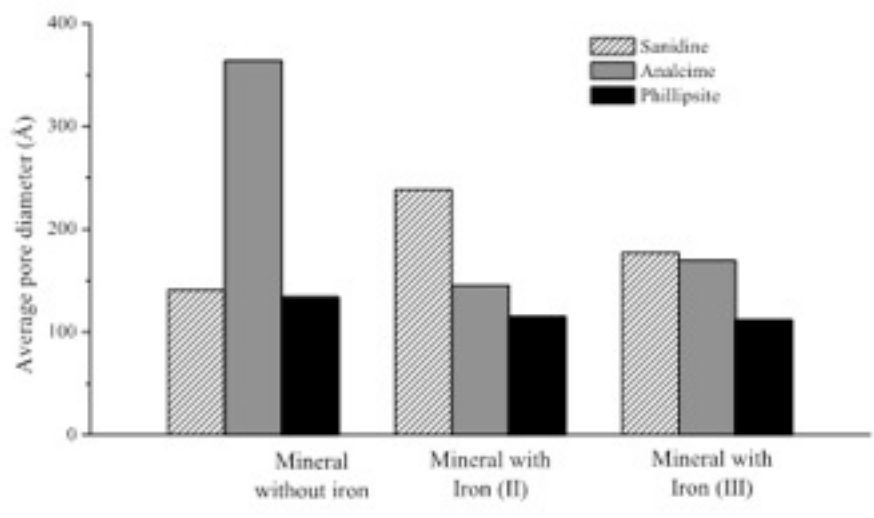
Volume of pores

4.2 - BET Pore surface area



Surface pore area

4.3 - BET Pore diameter



Average pore diameter